

# Noncompact Heisenberg spin magnets from high-energy QCD

## III. Quasiclassical approach

S.É. DERKACHOV<sup>1</sup>, G.P. KORCHEMSKY<sup>2</sup> and A.N. MANASHOV<sup>3\*</sup>

<sup>1</sup> *Department of Mathematics, St.-Petersburg Technology Institute,  
198013 St.-Petersburg, Russia*

<sup>2</sup> *Laboratoire de Physique Théorique<sup>†</sup>, Université de Paris XI,  
91405 Orsay Cédex, France*

<sup>3</sup> *Institut für Theoretische Physik II, Ruhr-Universität Bochum,  
44780 Bochum, Germany*

### Abstract:

The exact solution of the noncompact  $SL(2, \mathbb{C})$  Heisenberg spin magnet reveals a hidden symmetry of the energy spectrum. To understand its origin, we solve the spectral problem for the model within quasiclassical approach. In this approach, the integrals of motion satisfy the Bohr-Sommerfeld quantization conditions imposed on the orbits of classical motion. In the representation of the separated coordinates, the latter wrap around a Riemann surface defined by the spectral curve of the model. A novel feature of the obtained quantization conditions is that they involve both the  $\alpha$ - and  $\beta$ -periods of the action differential on the Riemann surface, thus allowing us to find their solutions by exploring the full modular group of the spectral curve. We demonstrate that the quasiclassical energy spectrum is in a good agreement with the exact results.

---

\* Permanent address: Department of Theoretical Physics, Sankt-Petersburg State University, 199034 St.-Petersburg, Russia

<sup>†</sup>Unite Mixte de Recherche du CNRS (UMR 8627)

# Contents

<b>1. Introduction</b>	<b>2</b>
<b>2. Noncompact Heisenberg spin magnet</b>	<b>6</b>
2.1. Classical model . . . . .	6
2.2. Quantum model . . . . .	7
<b>3. Quasiclassical wave function</b>	<b>8</b>
3.1. Properties of the WKB expansion . . . . .	9
3.2. Quantization conditions . . . . .	11
<b>4. Quasiclassical spectrum</b>	<b>14</b>
4.1. Baxter $Q$ -blocks . . . . .	14
4.2. Asymptotic solutions to the Baxter equation . . . . .	15
4.3. Energy spectrum . . . . .	18
<b>5. Solving the quantization conditions</b>	<b>19</b>
5.1. Lattice structure . . . . .	21
5.1.1. Special case: $N = 3$ . . . . .	23
5.1.2. Special case: $N = 4$ . . . . .	24
5.2. Whitham flow . . . . .	26
5.2.1. Whitham equations . . . . .	27
5.2.2. Whitham flow at $N = 3$ . . . . .	28
<b>6. Conclusions</b>	<b>33</b>
<b>A Appendix: Matching conditions</b>	<b>34</b>
<b>B Appendix: Calculation of the energy spectrum</b>	<b>36</b>
<b>C Appendix: Calculation of the quasimomentum</b>	<b>39</b>

# 1. Introduction

Exact solution of the spectral problem for quantum-mechanical multi-particle systems is the central problem in the theory of Integrable Lattice Models [1]. One of the best known examples of such systems is spin-1/2 Heisenberg spin magnet. The model can be solved exactly by the Algebraic Bethe Ansatz (ABA) and it has numerous applications [2, 3, 4]. The Heisenberg magnet model can be generalized from the compact  $SU(2)$  spins to noncompact spins, “living” in an infinite-dimensional, unitary representations of the  $SL(2, \mathbb{C})$  group. The corresponding integrable model describes a nearest-neighbour interaction between the  $SL(2, \mathbb{C})$  spins and is called the noncompact Heisenberg magnet [5].

The noncompact Heisenberg spin magnets have important implications in high-energy QCD [6, 7]. It is well-known that hadronic scattering amplitudes grow as a power of energy in agreement with the Regge model. In perturbative QCD framework, this behaviour can be attributed to a contribution of colour-singlet gluonic compound states. These states satisfy the Bartels-Kwiecinski-Praszalowicz equation which coincides, in the multi-colour limit, with the Schrödinger equation for the noncompact  $SL(2, \mathbb{C})$  spin magnet. The effective QCD interaction between  $N$  reggeized gluons ( $N = 2, 3, \dots$ ) occurs on two-dimensional plane of transverse degrees of freedom (the impact parameter space). It is described by the Hamiltonian  $\mathcal{H}_N$ , which defines a quantum-mechanical system of  $N$  particles with the coordinates  $\vec{z}_k = (x_k, y_k)$  and the momenta  $\vec{p}_k = -i\vec{\partial}_k$ , such that  $[z_k^\alpha, p_n^\beta] = i\delta_{kn}\delta^{\alpha\beta}$  ( $k, n = 1, \dots, N$  and  $\alpha, \beta = 1, 2$ ) with the Planck constant  $\hbar = 1$ . To map this system into a Heisenberg magnet, one introduces holomorphic,  $z = x + iy$ , and antiholomorphic,  $\bar{z} = x - iy$ , complex coordinates on the plane and defines the spin operators as

$$S_k^0 = iz_k p_k + s, \quad S_k^- = -ip_k, \quad S_k^+ = iz_k^2 p_k + 2sz_k. \quad (1.1)$$

Here  $p_k = -i\partial/\partial z_k$  is a (complex) momentum along the  $z$ -direction and the parameter  $s = (1 + n_s)/2 + i\nu_s$  (with  $n_s$  integer and  $\nu_s$  real) is a single-particle  $SL(2, \mathbb{C})$  spin. One also defines the antiholomorphic spin operators  $\vec{S}_k^0, \vec{S}_k^-$  and  $\vec{S}_k^+$  acting along the  $\bar{z}$ -direction. They are given by similar expressions with  $z_k$  and  $s$  replaced by  $\bar{z}_k = z_k^*$  and  $\bar{s} = 1 - s^* = (1 - n_s)/2 + i\nu_s$ , respectively. The operators  $\vec{S}_k$  and  $\vec{S}_n$  act along different directions on the  $\vec{z}$ -plane and therefore commute. They satisfy the standard  $sl(2)$  commutation relations

$$[S_k^+, S_n^-] = 2S_k^0 \delta_{kn}, \quad [S_k^0, S_n^\pm] = \pm S_k^\pm \delta_{kn}, \quad (1.2)$$

with the quadratic Casimir operator  $\vec{S}_n^2 = (S_n^0)^2 + (S_n^+ S_n^- + S_n^- S_n^+)/2 = s(s-1)$ . Similar relations hold in the antiholomorphic sector. Defined in this way, the spin operators  $\vec{S}_k$  and  $\vec{\bar{S}}_k$  are the generators of the unitary principal series representation of the  $SL(2, \mathbb{C})$  group labelled by the pair of spins  $(s, \bar{s})$ , or equivalently integer  $n_s$  and real  $\nu_s$  [8]. The interaction between  $N$  reggeized gluons in multi-colour QCD is translated into the nearest-neighbour interaction between the spins  $\vec{S}_k$  and  $\vec{\bar{S}}_k$  for the  $SL(2, \mathbb{C})$  Heisenberg magnet at  $s = 0$  and  $\bar{s} = 1$  [6, 7]

$$\mathcal{H}_N = \sum_{k=1}^N H_{k,k+1}, \quad H_{k,k+1} = H(\vec{S}_k \cdot \vec{S}_{k+1}) + H(\vec{\bar{S}}_k \cdot \vec{\bar{S}}_{k+1}), \quad (1.3)$$

where  $H_{N,N+1} = H_{N,1}$  and the two-particle Hamiltonian is expressed in terms of the Euler  $\psi$ -function,  $H(x) = \psi(j(x)) + \psi(1 - j(x)) - 2\psi(1)$  with  $j(j-1) = 2x + 2s(s-1)$ . As follows

from (1.3),  $\mathcal{H}_N$  can be split into a sum of two mutually commuting Hamiltonians acting along the  $z$ - and  $\bar{z}$ -directions.

The noncompact  $SL(2, \mathbb{C})$  Heisenberg magnet (1.3) is a completely integrable model. It possesses a large enough set of mutually commuting conserved charges  $q_n$  and  $\bar{q}_n$  ( $n = 2, \dots, N$ ) such that  $\bar{q}_n = q_n^\dagger$  and  $[\mathcal{H}_N, q_n] = [\mathcal{H}_N, \bar{q}_n] = 0$ . The charges  $q_n$  are polynomials of degree  $n$  in the holomorphic spin operators. They have a particular simple form at  $s = 0$  [6, 7]

$$q_n = \sum_{1 \leq j_1 < j_2 < \dots < j_n \leq N} z_{j_1 j_2} z_{j_2 j_3} \dots z_{j_n j_1} p_{j_1} p_{j_2} \dots p_{j_n} \quad (1.4)$$

with  $z_{jk} = z_j - z_k$  and  $p_j$  defined in (1.1). The “lowest” charge  $q_2$  is related to the total spin of the system  $h$ . For the principal series of the  $SL(2, \mathbb{C})$  it takes the following values [8]

$$q_2 = -h(h-1) + Ns(s-1), \quad h = \frac{1+n_h}{2} + i\nu_h, \quad (1.5)$$

with  $n_h$  integer and  $\nu_h$  real. The eigenvalues of the integrals of motion,  $q_2, \dots, q_N$ , form the total set of quantum numbers parameterizing the eigenstates of the model (1.3). As was already mentioned, at  $s = 0$  and  $\bar{s} = 1$  the latter define the multi-gluonic compound states in multi-colour QCD.

In spite of the fact that the noncompact  $SL(2, \mathbb{C})$  Heisenberg magnet represents a generalization of the compact  $SU(2)$  spin chain, a very little has been known about its energy spectrum till recently. One of the reasons is that the exact solution of the eigenproblem for the Hamiltonian (1.3) represents a difficulty of principle. In distinction with the compact magnets, the quantum space of the  $SL(2, \mathbb{C})$  magnet does not possess the highest weight and, as a consequence, the conventional methods like the ABA method [2, 4] are not applicable.

The eigenproblem for the noncompact  $SL(2, \mathbb{C})$  Heisenberg magnet has been solved exactly in Refs. [5, 9, 10] using the method the Baxter  $\mathbb{Q}$ -operator [1]. This method allowed us to establish the quantization conditions for the integrals of motion of the model,  $q_3, \dots, q_N$ , obtain an explicit form of the dependence of the energy on the integrals of motion,  $E_N = E_N(\nu_h, n_h, q_3, \dots, q_N)$ , and construct the corresponding eigenfunctions in the representation of the Separated Variables [11]. Solving the quantization conditions, we calculated the spectrum of the noncompact  $SL(2, \mathbb{C})$  magnet of spin  $s = 0$  for the number of particles  $2 \leq N \leq 8$ . Its close examination revealed the following properties of the model [10]:

- Quantized values of the charges  $q_k$  (with  $k = 3, \dots, N$ ) depend on the “hidden” set of integers  $\boldsymbol{\ell} = (\ell_1, \ell_2, \dots, \ell_{2(N-2)})$

$$q_k = q_k(\nu_h; n_h, \boldsymbol{\ell}), \quad (1.6)$$

where integer  $n_h$  and real  $\nu_h$  define the total  $SL(2, \mathbb{C})$  spin of the state, Eq. (1.5).

- As a function of continuous  $\nu_h$ , the charges form the family of trajectories in the moduli space  $\mathbf{q} = (q_2, q_3, \dots, q_N)$  labelled by integers  $n_h$  and  $\boldsymbol{\ell}$ . Each trajectory in the  $q$ -space induces the corresponding trajectory for the energy  $E_N$  (see Figure 2 below)

$$E_N = E_N(\nu_h; n_h, \boldsymbol{\ell}). \quad (1.7)$$

- For fixed total  $SL(2, \mathbb{C})$  spin of the model, Eq. (1.5), the eigenvalues of the “highest” charge  $q_N^{1/N}$  define an infinite set of distinct points on the complex  $q_N^{1/N}$ -plane. At  $N = 3$  and  $N = 4$  they are located close to the vertices of a lattice built from equilateral triangles and squares, respectively (see Figures 4 and 5 below).

Their origin remains obscure mainly due to a rather complicated form of the exact quantization conditions. The main goal of this paper is to present a physical interpretation of these properties. Our analysis is based on a generalization of the well-known quasiclassical methods to noncompact Heisenberg magnets. One might expect *a priori* that these methods could be applicable only for high excited states. Nevertheless, as we will demonstrate below, the quasiclassical formulae work with a good accuracy throughout the whole spectrum of the noncompact  $SL(2, \mathbb{C})$  Heisenberg magnet.

To formulate the quasiclassical solution of the eigenproblem for Hamiltonian (1.3), one has to consider a classical analog of the noncompact Heisenberg spin magnet [12, 13]. From point of view of classical dynamics, the model describes a chain of  $N$  interacting particles on the two-dimensional  $\vec{z}$ -plane. We use (anti)holomorphic variables on the phase space and define the coordinates and the momenta of particles as  $\vec{z}_k = (z_k, \bar{z}_k)$  and  $\vec{p}_k = (p_k, \bar{p}_k)$ , respectively. By the definition,  $z_k$  and  $p_k$  take complex values such that  $\bar{z}_k = z_k^*$  and  $\bar{p}_k = p_k^*$ .<sup>1</sup> The only non-trivial Poisson bracket is given by  $\{z_k, p_n\} = \{\bar{z}_k, \bar{p}_n\} = \delta_{kn}$ . The classical model inherits a complete integrability of the quantum noncompact spin magnet. Its Hamiltonian and the integrals of motion are obtained from (1.3), (1.1) and (1.4) by replacing the momentum operators by the corresponding classical functions leading to  $\{q_k, \mathcal{H}_N\} = \{q_k, q_n\} = 0$ . Since the Hamiltonian (1.3) is given by the sum of holomorphic and antiholomorphic functions, from point of view of classical dynamics the model describes two copies of one-dimensional systems “living” on the complex  $z$ - and  $\bar{z}$ -lines. The solutions to the classical equations of motion have a rich structure and turn out to be intrinsically related to the finite-gap solutions to the soliton equations [14, 15]. Namely, the classical trajectories have the form of soliton waves propagating in the chain of  $N$  particles. Their explicit form in terms of the Riemann  $\theta$ -functions was established in [12] by the methods of the finite-gap theory [14, 15]. The charges  $\mathbf{q}$  define the moduli of the soliton solutions and take arbitrary complex values in the classical model. Going over to the quantum model, one finds that  $\mathbf{q}$  are quantized. In the quasiclassical approach presented in this paper, their values satisfy the Bohr–Sommerfeld quantization conditions imposed on the orbits of classical motion of  $N$  particles.

In a standard manner, the WKB ansatz for the eigenfunction of the model (1.3) involves the “action” function,  $\Psi_{\text{WKB}}(\vec{z}_1, \dots, \vec{z}_N) \sim \exp(iS_0/\hbar)$ . Due to complete integrability of the classical system, it can be defined as a simultaneous solution to the system of the Hamilton–Jacobi equations

$$\sum_{k=1}^N \frac{\partial S_0}{\partial z_k} = P, \quad q_n \left( \mathbf{z}, \frac{\partial S_0}{\partial \mathbf{z}} \right) = q_n, \quad (n = 2, \dots, N), \quad (1.8)$$

where  $\mathbf{z} = (z_1, \dots, z_N)$  denotes the set of holomorphic coordinates,  $q_n(\mathbf{z}, \mathbf{p})$  stands for the symbol of the operator (1.4) and  $P$  is a holomorphic component of the total momentum of  $N$  particles. The  $\bar{z}$ -dependence of  $S_0$  is constrained by similar relations in the antiholomorphic sector. To find a general solution to Eq. (1.8), one performs a canonical transformation to the classical separated coordinates [11, 14]

$$(\vec{z}_1, \vec{z}_2, \dots, \vec{z}_N) \xrightarrow{\text{SoV}} (\vec{z}_0, \vec{x}_1, \vec{x}_2, \dots, \vec{x}_{N-1}), \quad (1.9)$$

---

<sup>1</sup>Of course, one can work instead with real, Cartesian coordinates, but our choice is advantageous as it is dictated by the chiral structure of the Hamiltonian (1.3).

with  $\vec{z}_0$  the center-of-mass coordinate of the system and  $\vec{x}_n = (x_n, \bar{x}_n = x_n^*)$  new collective (separated) coordinates. As explained in Section 2.1, the classical dynamics in the separated variables is determined by the spectral curve (“equal energy” condition)

$$\Gamma_N : \quad y^2 = t_N^2(x) - 4x^{2N}, \quad t_N(x) = 2x^N + q_2x^{N-2} + \dots + q_{N-1}x + q_N, \quad (1.10)$$

with  $y(x) = 2x^N \sinh p_x$  and  $p_x$  being the momentum in the separated coordinates. Here  $t_N(x)$  is a polynomial of degree  $N$  with the coefficients defined by the holomorphic integrals of motion  $q_n$ . The spectral curve establishes the relation between the holomorphic components of the separated coordinates,  $x$  and  $p_x$ , for a given set of the “energies”  $q_2, \dots, q_N$ . As we will see below, its properties play the central rôle in our analysis.

In the separated coordinates, the solution to the Hamilton-Jacobi equations (1.8) takes the form  $S_0(\vec{z}_0, \vec{x}_1, \vec{x}_2, \dots, \vec{x}_{N-1}) = (\vec{P} \cdot \vec{z}_0) + \sum_{k=1}^{N-1} S_0(\vec{x}_k)$  with [14]

$$S_0(\vec{x}) = \int_{x_0}^x dx p_x + \int_{\bar{x}_0}^{\bar{x}} d\bar{x} \bar{p}_{\bar{x}} = 2 \operatorname{Re} \int_{x_0}^x dx p_x. \quad (1.11)$$

Here complex momentum  $\bar{p}_{\bar{x}} = p_x^*$  was defined in (1.10) and  $\vec{x}_0$  is arbitrary. The WKB expression for the wave function in the separated coordinates,  $\sim \exp(iS_0(\vec{z}_0, \vec{x}_1, \vec{x}_2, \dots, \vec{x}_{N-1})/\hbar)$ , factorizes into a product of single-particle wave functions,  $Q_{\text{WKB}}(\vec{x}_k) \sim \exp(iS_0(\vec{x}_k)/\hbar)$ . According to (1.10), the momentum,  $p_x$ , and, as a consequence, the action function  $S_0(\vec{x})$  are multi-valued functions of  $x$ . Denoting the different branches of the action function as  $S_{0,\alpha}(\vec{x})$ , one writes the WKB expression for the wave function of the quantum spin magnet as a sum over branches [16, 17]

$$Q_{\text{WKB}}(\vec{x}) = \sum_{\alpha} A_{\alpha}(\vec{x}) \exp\left(\frac{i}{\hbar} S_{0,\alpha}(\vec{x})\right). \quad (1.12)$$

The function  $A_k(\vec{x})$  takes into account subleading WKB corrections and is uniquely fixed by  $S_{0,\alpha}(\vec{x})$ . In general, the expression in the r.h.s. of (1.12) is not a single-valued function of  $\vec{x}$ . For  $Q_{\text{WKB}}(\vec{x})$  to be well-defined, the charges  $\mathbf{q}$  have to satisfy the Bohr-Sommerfeld quantization conditions. One of the main results in this paper is that these conditions can be expressed in terms of the periods of the “action” differential over the canonical set of the  $\alpha$ - and  $\beta$ -cycles on the Riemann surface corresponding to the complex curve (1.10)

$$\operatorname{Re} \oint_{\alpha_k} dx p_x = \pi \hbar \ell_{2k-1}, \quad \operatorname{Re} \oint_{\beta_k} dx p_x = \pi \hbar \ell_{2k}, \quad (k = 1, \dots, N-2), \quad (1.13)$$

with  $\ell = (\ell_1, \dots, \ell_{2N-4})$  being the set of integers.

The relations (1.13) define the system of  $2(N-2)$  real equations on the  $(N-2)$  complex charges  $q_3, \dots, q_N$  (we recall that the eigenvalues of the “lowest” charge  $q_2$  are given by (1.5)). Their solutions lead to the quasiclassical expressions for the eigenvalues of the integrals of motion of the noncompact spin magnet. As we will demonstrate in Section 5, these expressions have the form (1.6) and are in a good agreement with the exact results of Ref. [9, 10]. A novel feature of the quantization conditions (1.13) is that they involve *both* the  $\alpha$ - and  $\beta$ -periods on the Riemann surface. This should be compared with the situation in one-dimensional lattice integrable models, like the Toda chain model [16, 18] and the  $SL(2, \mathbb{R})$  Heisenberg spin magnet [19, 20, 21]. There, the WKB quantization conditions involve only the  $\alpha$ -cycles, since the  $\beta$ -cycles correspond to classically forbidden zones. In the  $SL(2, \mathbb{C})$  spin magnet, the classical trajectories wrap over an

arbitrary closed contour on the spectral curve (1.10) leading to (1.13). This fact allows one to explore the full modular group [22] of the complex curve (1.10).

The paper is organized as follows. In Section 2 we remind the definition of the noncompact Heisenberg spin magnet both in the classical and quantum cases. Going over to the representation of the Separated Variables we construct the wave function of the model in terms of the solutions to the Baxter equation. Applying the WKB methods, we solve the Baxter equation in Section 3 and show that the quasiclassical expression for the wave function is uniquely defined by the complex curve  $\Gamma_N$  introduced in (1.10). Requiring this function to be single-valued, we obtain the quantization conditions (1.13) for the integrals of motion  $q_n$ . In Section 4 we obtain quasiclassical expressions for the energy and the quasimomentum. Both observables are expressed in terms of the  $Q$ -blocks, which satisfy the holomorphic Baxter equation and have prescribed analytical properties and asymptotic behaviour at infinity. In Section 5 we analyze the quantization conditions (1.13) and compare their solutions with the exact results for the energy spectrum. Section 6 contains concluding remarks. Some technical details of the calculations are summarized in two Appendices.

## 2. Noncompact Heisenberg spin magnet

Let us summarize, following [12, 13], the main features of the  $SL(2, \mathbb{C})$  Heisenberg spin magnet in the classical and quantum mechanics.

### 2.1. Classical model

In the classical case, the model describes the chain of  $N$  interacting particles on the two-dimensional plane with the Hamiltonian (1.3). The classical motion along the complex  $z$ -direction is described by the Hamilton equations

$$\partial_t z_k = \{z_k, \mathcal{H}_N\} = \frac{\partial \mathcal{H}_N}{\partial p_k}, \quad \partial_t p_k = \{p_k, \mathcal{H}_N\} = -\frac{\partial \mathcal{H}_N}{\partial z_k}. \quad (2.1)$$

This system is completely integrable and the integrals of the motion are given by (1.4). Following the Quantum Inverse Scattering Method [2], one can describe the classical Heisenberg spin magnet by the Lax matrix

$$L_k(u) = u \cdot \mathbb{1} + iS_k^0 \cdot \sigma^3 + iS_k^+ \cdot \sigma^- + iS_k^- \cdot \sigma^+ = \begin{pmatrix} u + iS_k^0 & iS_k^- \\ iS_k^+ & u - iS_k^0 \end{pmatrix}, \quad (2.2)$$

with  $\sigma^a$  being the Pauli matrices. The dynamical variables  $S_k^0$ ,  $S_k^-$  and  $S_k^+$  depend on the (holomorphic) coordinates and momenta of particles,  $z_k$  and  $p_k$ , respectively, and they are given by the same expressions as in (1.1). The Hamilton equations (2.1) are equivalent to the matrix Lax pair relation

$$\partial_t L_k(u) = \{L_k(u), \mathcal{H}_N\} = A_{k+1}(u)L_k(u) - L_k(u)A_k(u), \quad (2.3)$$

with  $A_k(u)$  being a  $2 \times 2$  matrix depending on the coordinates and momenta of particles.

The exact integration of the classical equations of motion is based on the Baker-Akhiezer function  $\Psi_k(u; t)$  [15]. By the definition, it satisfies the system of matrix relations

$$L_k(u)\Psi_k(u; t) = \Psi_{k+1}(u; t), \quad \partial_t \Psi_k(u; t) = A_k(u)\Psi_k(u; t). \quad (2.4)$$

Introducing the monodromy matrix as a consecutive product of the Lax matrices, one finds that it produces the shift of the Baker-Akhiezer function along the chain

$$T_N(u) = L_N(u) \dots L_1(u), \quad T_N(u)\Psi_1(u; t) = \Psi_{N+1}(u; t). \quad (2.5)$$

For periodic boundary conditions,  $z_{k+N} = z_k$  and  $p_{k+N} = p_k$ , the Baker-Akhiezer function satisfies the Bloch-Floquet relation

$$\Psi_{N+k}(u; t) = w(u)\Psi_k(u; t), \quad (2.6)$$

According to (2.5), the Bloch-Floquet factor  $w(u)$  is an eigenvalue of the monodromy matrix. Therefore, it does not depend on the time and satisfies the characteristic equation

$$\det(T_N(u) - w) = w^2 - w t_N(u) + u^{2N} = 0. \quad (2.7)$$

Here  $t_N(u) = \text{tr } T_N(u)$  is a polynomial in  $u$  of degree  $N$  with the coefficients given by the integrals of motion, Eq. (1.10). Introducing the complex function  $y(u) = w - u^{2N}/w$ , one obtains from (2.7) that  $y(u)$  defines the algebraic complex curve (1.10).

The Baker-Akhiezer function  $\Psi_k(u; t)$  is a double-valued function on the complex  $u$ -plane [15]. Its explicit expression in terms of the theta-functions defined on the curve (1.10) can be found in [12]. We do not present it here since we will not use the Baker-Akhiezer function in the rest of the paper. The function  $\Psi_k(u; t)$  has  $N - 1$  simple poles at  $u = x_k$  ( $k = 1, \dots, N - 1$ ) and the same number of zeros. Remarkable property of its poles is that the variables  $(x_k, p(x_k))$  (with  $p(u) = \ln(w(u)/u^N)$  and  $k = 1, \dots, N - 1$ ) form the set of holomorphic separated variables for the classical model, Eq. (1.9). Notice that  $x_k$  and  $p(x_k)$  take arbitrary complex values. This allows one to integrate the equations of motion exactly and reconstruct the classical trajectories of particles on the Riemann surface defined by the curve (1.10). The same classical motion describes a soliton wave propagating in the chain of  $N$  particles on the two-dimensional  $\bar{z}$ -plane.

## 2.2. Quantum model

In the quantum case, the eigenfunction of the  $SL(2, \mathbb{C})$  Heisenberg spin magnet,  $\Psi(\vec{z}_1, \dots, \vec{z}_N)$ , is defined as a simultaneous eigenstate of the integrals of motion  $q_2, \dots, q_N$ , Eq. (1.4), and their antiholomorphic counterparts. Together with the total momentum of the system,  $\vec{P}$ , their eigenvalues  $q = (q_2, \dots, q_N)$  define the total set of the quantum numbers of the model. Due to chiral structure of the Hamiltonian and the integrals of motion, the eigenfunction can be decomposed as [23]

$$\Psi(\vec{z}_1, \dots, \vec{z}_N) = \sum_{a, b} C_{ab}(q, \bar{q}) \Psi_q^{(a)}(z_1, \dots, z_N) \overline{\Psi}_{\bar{q}}^{(b)}(\bar{z}_1, \dots, \bar{z}_N), \quad (2.8)$$

where  $\Psi_q^{(a)}$  and  $\overline{\Psi}_{\bar{q}}^{(b)}$  diagonalize the integrals of motion in the holomorphic and antiholomorphic sectors, respectively, and  $C_{ab}$  are mixing coefficients. The function  $\Psi(\vec{z}_1, \dots, \vec{z}_N)$  is a single-valued function on the two-dimensional plane. It belongs to the principal series of the  $SL(2, \mathbb{C})$  group labelled by the spins  $(h, \bar{h})$  defined in (1.5) (with  $\bar{h} = 1 - h^*$ ) and is normalizable with respect to the  $SL(2, \mathbb{C})$  scalar product. In contrast with  $\Psi(\vec{z}_1, \dots, \vec{z}_N)$ , the chiral solutions  $\Psi_q^{(a)}$  and  $\overline{\Psi}_{\bar{q}}^{(b)}$  acquire nontrivial monodromy when  $\vec{z}_k$  encircles other particles on the plane. The quantization conditions for the integrals of motion  $\mathbf{q}$  follow from the requirement that the monodromy should



cancel in the r.h.s. of (2.8). The same condition fixes (up to an overall normalization) the mixing coefficients  $C_{ab}$ .

To formulate the quantization conditions it is convenient to switch from the coordinate  $\vec{z}$ -representation to the representation of the Separated Variables (SoV) [11]. In this representation, the wave function takes a factorized form

$$\Psi(\vec{z}_1, \vec{z}_2, \dots, \vec{z}_N) \xrightarrow{\text{SoV}} \Phi(\vec{z}_0, \vec{x}_1, \vec{x}_2, \dots, \vec{x}_{N-1}) = e^{i\vec{P}\cdot\vec{z}_0} Q(\vec{x}_1) Q(\vec{x}_2) \dots Q(\vec{x}_N), \quad (2.9)$$

where  $\vec{P}$  is the total momenta of  $N$  particles,  $\vec{z}_0$  is the center-of-mass coordinate of the system and  $\vec{x}_1, \dots, \vec{x}_{N-1}$  are new collective (separated) coordinates. The explicit form of the unitary transformation to the SoV representation can be found in [5] (see also [24] for similar expressions at  $N = 2$  and  $N = 3$ ). The eigenfunction in the SoV representation has the following properties. Introducing holomorphic and antiholomorphic components  $\vec{x} = (x, \bar{x})$ , one finds that the possible values of the separated coordinates can be parameterized by integer  $n$  and real  $\nu$  as

$$x = \nu - \frac{in}{2}, \quad \bar{x} = \nu + \frac{in}{2}, \quad (2.10)$$

so that  $\bar{x} = x^*$  and  $i(x - \bar{x}) = n$ . Here, as before, one has  $\hbar = 1$ . To restore the  $\hbar$ -dependence one has to substitute  $n \rightarrow \hbar n$ . Notice that, in contrast with the classical case, the separated variables have a discrete imaginary part for finite  $\hbar$ .

A single-particle  $Q$ -function entering (2.9) satisfies the holomorphic Baxter equation

$$(x + is)^N Q(x + i, \bar{x}) + (x - is)^N Q(x - i, \bar{x}) = t_N(x) Q(x, \bar{x}), \quad (2.11)$$

with  $t_N(x)$  defined in (1.10). Similar equation holds for  $Q(x, \bar{x})$  in the antiholomorphic sector with  $s$  and  $q_n$  replaced by  $\bar{s} = 1 - s^*$  and  $\bar{q}_n = q_n^*$ , respectively. The solution to the Baxter equations,  $Q(\nu - in/2, \nu + in/2)$ , is a well-defined, regular function of integer  $n$  and real  $\nu$ . At large  $\nu$  and fixed  $n$  it has the following asymptotic behaviour

$$Q(\nu - in/2, \nu + in/2) \sim e^{i\Theta} \nu^{h+\bar{h}-N(s+\bar{s})} + e^{-i\Theta} \nu^{1-h+1-\bar{h}-N(s+\bar{s})}, \quad (2.12)$$

where  $h$  and  $\bar{h} = 1 - h^*$  define the total  $SL(2, \mathbb{C})$  spin of the model, Eq. (1.5), and  $\Theta$  is some phase.

The exact solution to Eqs. (2.11) and (2.12) was constructed in Refs. [9, 10]. It allowed us to establish the quantization conditions for the integrals of motion and calculate the energy spectrum of the model. In this paper we shall present another, quasiclassical approach to solving the Baxter equations. Although it does not provide the exact solution for the  $Q$ -function, it allows us to elucidate a hidden symmetry of the energy spectrum.

### 3. Quasiclassical wave function

The quasiclassical approach relies on the observation that the holomorphic Baxter equation (2.11) resembles a one-dimensional discrete Schrödinger equation. A specific feature of the model is that  $x$ -coordinates entering the Baxter equation takes complex values (2.10) and the Planck constant equals unity  $\hbar = 1$ .<sup>2</sup> As a consequence, the quasiclassical limit corresponds to large values of the “energies”  $q_2, \dots, q_N$  in Eq. (1.10).

---

<sup>2</sup>In quantum models, like the Toda chain, the Planck constant controls a shift of the argument of the  $Q$ -function in the l.h.s. of the Baxter equation (2.11).

To perform the large  $\mathbf{q}$ -limit in (2.11), one introduces an arbitrary auxiliary parameter  $\eta$  and rescales simultaneously the coordinates,  $x \rightarrow x/\eta$ , and the charges,  $q_k \rightarrow q_k \eta^k$ . Defining

$$\widehat{t}_N(x) = \eta^N t_N(x/\eta) = 2x^N + \widehat{q}_2 x^{N-2} + \dots + \widehat{q}_N, \quad (3.1)$$

with  $\widehat{q}_n \equiv q_n \eta^n = \mathcal{O}(\eta^0)$  as  $\eta \rightarrow 0$ , one finds that this transformation allows one to get rid of large parameters in the Baxter equation (2.11). At the same time, it sets the Planck constant as  $\hbar = \eta$ . Let us look for the solution to the holomorphic Baxter equation in the WKB form [16, 17]

$$Q(x/\eta) = \exp\left(\frac{i}{\eta} \int_{x_0}^x dx S'(x)\right), \quad S(x) = S_0(x) + \eta S_1(x) + \mathcal{O}(\eta^2), \quad (3.2)$$

where  $S'(x) = dS(x)/dx$  and  $x_0$  is an arbitrary reference point. Its substitution into (2.11) leads to the following relations

$$2 \cosh S'_0(x) = \frac{\widehat{t}_N(x)}{x^N}, \quad S'_1(x) = \frac{i}{2} (\ln \sinh S'_0(x))' + \frac{isN}{x}. \quad (3.3)$$

One can systematically improve the WKB expansion (3.2) and express subleading corrections to  $S(x)$  in terms of the leading term  $S_0(x)$ . Similar expressions can be obtained for solutions to the antiholomorphic Baxter equation  $\overline{Q}(\bar{x})$ . Then, a general WKB expression for  $Q(x, \bar{x})$  is given by a bilinear combination of  $Q(x)$  and  $\overline{Q}(\bar{x})$ .

### 3.1. Properties of the WKB expansion

Introducing notation for

$$p_x = S'_0(x), \quad y(x) = 2x^N \sinh p_x, \quad (3.4)$$

one rewrites the first relation in (3.3) as

$$y^2(x) = \widehat{t}_N^2(x) - 4x^{2N}. \quad (3.5)$$

We notice that, up to rescaling of parameters,  $y(x)$  coincides with the hyperelliptic curve  $\Gamma_N$ , Eq. (1.10). The coincidence is not accidental of course. The leading term of the WKB expansion,  $S_0(x)$ , satisfies the classical Hamilton-Jacobi equations in the separated coordinates. Its derivative,  $p_x = S'_0(x)$ , defines a (complex-valued) holomorphic component of the momentum in the separated variables. As such, it belongs to the spectral curve of the classical model (2.7) for  $w(x) = x^N \exp(p_x)$ .

The leading term of the WKB expansion (3.2) can be calculated as

$$S_0(x) = \int_{x_0}^x dx p_x = \int_{x_0}^x \frac{dx}{y(x)} [N \widehat{t}_N(x) - x \widehat{t}'_N(x)] + x p_x \Big|_{x_0}^x. \quad (3.6)$$

Solving (3.5) we find that  $y(x)$  and, as a consequence  $S'_0(x)$ , are double-valued functions on the complex  $x$ -plane. To specify two branches of  $S'_0(x)$ , one makes cuts on the  $x$ -plane in an arbitrary way between the  $2(N-1)$  branching points  $\sigma_j$ . The latter are defined as  $y(\sigma_j) = 0$ , or equivalently

$$\widehat{t}_N^2(\sigma_j) - 4\sigma_j^{2N} = (\widehat{q}_2 \sigma_j^{N-2} + \dots + \widehat{q}_N)(4\sigma_j^N + \widehat{q}_2 \sigma_j^{N-2} + \dots + \widehat{q}_N) = 0. \quad (3.7)$$

According to their definition, the branching points correspond to the special points on the phase space of the classical system, in which the holomorphic component of the momentum (in the separated coordinates) takes the values  $p_x = 0$  and  $p_x = \pm i\pi$ . Two different solutions to (3.5) give rise to two branches  $S_{0,+}(x)$  and  $S_{0,-}(x)$  which are continuous functions of complex  $x$  except across the cuts. These functions are transformed one into another as  $x$  encircles the branching point  $\sigma_j$  in the anticlockwise direction

$$S'_{0,\pm}(x) \xrightarrow{x \circlearrowleft \sigma_j} -S'_{0,\mp}(x). \quad (3.8)$$

Their asymptotic behaviour at infinity can be found from (3.6) and (3.5) as

$$S'_{0,\pm}(x) \sim \pm \frac{\widehat{q}_2^{1/2}}{x} \sim \pm \frac{i}{x} \eta (h - 1/2), \quad (3.9)$$

as  $x \rightarrow \infty$ . Here, in the last relation, we replaced  $\widehat{q}_2 = q_2 \eta^2$  by its expression, Eq. (1.5), and took the limit  $\eta \rightarrow 0$  with  $|\eta(h - 1/2)| = |\eta(i\nu_h + n_h/2)| = \text{fixed}$ . Notice that the integration contour in (3.6) does not cross the cuts.

It becomes convenient to combine the two branches  $S'_{0,\pm}(x)$  and define  $S'_0(x)$  as a single-valued function on the Riemann surface  $\Gamma_N$  obtained by gluing together two copies of the  $x$ -plane along the  $(N - 1)$ -cuts  $[\sigma_{2j}, \sigma_{2j+1}]$  running between the branching points. By the definition,  $S'_0(x) = S'_{0,+}(x)$  on one plane (upper sheet) and  $S'_0(x) = S'_{0,-}(x)$  on another one (lower sheet). Then, it follows from Eq. (3.6) that  $dx S'_0(x)$  is a well-defined, meromorphic differential on  $\Gamma_N$  of the third kind (the dipole differential). It has a pair of poles located above the point  $x = \infty$  on the upper and lower sheets,  $P_\infty^+$  and  $P_\infty^-$ , respectively. Here we used the standard notation for the points on the Riemann surface,  $P_x^\pm = (x, \pm)$ .

Substituting (3.6) into (3.3), we calculate the first nonleading WKB correction as

$$S'_1(x) = \frac{i}{2} \left( \ln \frac{y(x)}{2x^N} \right)' + \frac{iNs}{x} = \frac{i}{4} \sum_{j=1}^{2N-2} \frac{1}{x - \sigma_j} + \frac{iN}{x} \left( s - \frac{1}{2} \right). \quad (3.10)$$

In distinction with the leading  $S_0$ -term, the function  $S'_1(x)$  is well-defined on the complex  $x$ -plane. Therefore, it takes the same value on the both sheets of the Riemann surface  $\Gamma_N$  and its asymptotic behaviour for  $x \rightarrow \infty$  is given by

$$S'_1(x) \sim \frac{i}{x} \left( Ns - \frac{1}{2} \right). \quad (3.11)$$

Combining together (3.6) and (3.10) we find that the two different branches  $S'_{0,\pm}(x)$ , or equivalently two different sheets of the Riemann surface  $\Gamma_N$ , give rise to two independent WKB solutions to the holomorphic Baxter equation (2.11)

$$Q_\pm(x/\eta) = \exp \left( \frac{i}{\eta} \int_{x_0}^x dx S'_\pm(x) \right), \quad S'_\pm = S'_{0,\pm}(x) + \eta S'_1(x) + \mathcal{O}(\eta^2). \quad (3.12)$$

Their asymptotics at infinity can be obtained from (3.9) and (3.11) as

$$Q_+(x/\eta) \sim x^{1-h-Ns}, \quad Q_-(x/\eta) \sim x^{h-Ns}, \quad (3.13)$$

as  $x \rightarrow \infty$ . Going over through similar analysis of the antiholomorphic Baxter equation, one arrives at the WKB expressions for  $\overline{Q}_\pm(\bar{x}/\eta)$ . They can be obtained from (3.12) by replacing holomorphic variables by their counterparts in the antiholomorphic sector. In this way, one gets from (3.13)

$$\overline{Q}_+(\bar{x}/\eta) \sim \bar{x}^{1-\bar{h}-N\bar{s}}, \quad \overline{Q}_-(\bar{x}/\eta) \sim \bar{x}^{\bar{h}-N\bar{s}}, \quad (3.14)$$

where  $\bar{x} = x^*$ ,  $\bar{s} = 1 - s^*$  and  $\bar{h} = 1 - h^*$ .

### 3.2. Quantization conditions

Let us construct the quasiclassical solution to the Baxter equation (2.11) as a bilinear combination of the chiral solutions  $Q_\pm(x/\eta)$  and  $\overline{Q}_\pm(\bar{x}/\eta)$

$$Q(x/\eta, \bar{x}/\eta) = c_+ Q_+(x/\eta) \overline{Q}_+(\bar{x}/\eta) + c_- Q_-(x/\eta) \overline{Q}_-(\bar{x}/\eta). \quad (3.15)$$

Using (3.13) and (3.14) one verifies that the wave function defined in this way has correct asymptotic behaviour at infinity, Eq. (2.12). The cross-terms  $Q_\pm \overline{Q}_\mp$  do not enter (3.15) since they do not verify (2.12). The functions  $Q_\pm(x/\eta)$  and  $\overline{Q}_\pm(\bar{x}/\eta)$  depend on the reference point  $x_0$ , Eq. (3.12), whereas  $Q(x/\eta, \bar{x}/\eta)$  should not depend on the choice of  $x_0$ . This fixes the  $x_0$ -dependence of the coefficients  $c_\pm(x_0)$  as ( $\bar{x}_0 = x_0^*$ )

$$c_\pm(x'_0) = c_\pm(x_0) \exp \left( \frac{i}{\eta} \left[ \int_{x_0}^{x'_0} dx S'_\pm(x) + \int_{\bar{x}_0}^{\bar{x}'_0} d\bar{x} \bar{S}'_\pm(\bar{x}) \right] \right). \quad (3.16)$$

By the construction, the WKB formula (3.15) is valid for small  $\eta$  and  $x \sim \eta^0$ . It describes the wave function,  $Q(x, \bar{x})$ , for large values of the separated coordinates,  $x \sim \bar{x} \sim 1/\eta$ , or equivalently  $n \sim \nu \sim 1/\eta$  in the parameterization (2.10). In this region, one can ignore the fact that  $n$  takes strictly integer values and treat the separated coordinates  $x$  and  $\bar{x}$  as continuous complex, mutually conjugated variables,  $\bar{x} = x^*$ . We recall that in one-dimensional lattice models, the Toda chain [16, 18] and the  $SL(2, \mathbb{R})$  magnet [19, 20, 21], the classical motion in the separated coordinates is restricted to finite intervals on the real  $x$ -axis. The WKB wave function is a continuous, single-valued function of real  $x$ , oscillating inside these intervals and vanishing at infinity. Going back to the noncompact  $SL(2, \mathbb{C})$  magnet, one finds that, in distinction with the models mentioned above, the classical motion in the separated coordinates occurs on the whole two-dimensional  $\vec{x}$ -plane. This suggests that the WKB wave function  $Q(x, \bar{x} = x^*)$  has to be well-defined on the complex  $x$ -plane. In particular, contrary to the chiral solutions to the Baxter equation (3.8), it should have a trivial monodromy around the branching points  $\sigma_j$ . In other words,  $Q(x, x^*)$  has to be a single-valued function on the complex  $x$ -plane rather than on the Riemann surface  $\Gamma_N$ . The former condition is much stronger than the latter one and, as we will show below, it leads to the WKB quantization conditions for the integrals of motion  $\mathbf{q}$ .

Let us examine the monodromy of the chiral solutions to the Baxter equation,  $Q_\pm(x/\eta)$ , around the branching points  $\sigma_j$ , Eq. (3.7). Encircling the branching point  $\sigma_j$  on the  $x$ -complex plane, one finds that the leading WKB term  $S'_0(x)$  is transformed according to (3.8) while the subleading term  $S'_1(x)$  stays invariant. Let us explore a freedom in choosing the reference point  $x_0$  in (3.12) and put  $x_0 = \sigma_j$  in order to ensure that  $S_\pm(\sigma_j) = 0$ . Then, it follows from (3.8) and (3.12) that the WKB solutions  $Q_\pm(x)$  defined in this way are transformed one into another as  $x$  encircles  $\sigma_j$  on the complex plane

$$Q_\pm(x/\eta) \xrightarrow{x \circlearrowleft \sigma_j} Q_\mp(x/\eta), \quad (\text{for } x_0 = \sigma_j). \quad (3.17)$$

Similar relations hold for the antiholomorphic solutions  $\overline{Q}_\pm(\bar{x}/\eta)$  at  $\bar{x}_0 = \bar{\sigma}_j \equiv \sigma_j^*$ . We find from (3.15) that  $Q(x/\eta, \bar{x}/\eta)$  stays invariant under this transformation provided that

$$c_+(\sigma_j) = c_-(\sigma_j), \quad (j = 1, 2, \dots, 2(N-1)). \quad (3.18)$$

These conditions ensure that the quasiclassical wave function (3.15) is a single-valued function on the complex  $x$ -plane. We recall that the branching points are defined as solutions to Eq. (3.7).

For different  $x_0$ , the coefficients  $c_\pm(x_0)$  are related to each other according to (3.16). Therefore, choosing  $x'_0 = \sigma_j$  and  $x_0 = 0$  we obtain from Eqs. (3.16) and (3.18)

$$\frac{c_+(0)}{c_-(0)} = \exp\left(\frac{2i}{\eta} \operatorname{Re} \int_0^{\sigma_j} dx [S'_{0,-}(x) - S'_{0,+}(x)] + \mathcal{O}(\eta)\right), \quad (3.19)$$

where  $j = 1, \dots, 2(N-1)$  and the integration contour does not cross the cuts on the complex  $x$ -plane. In arriving at (3.19), we applied (3.12) and took into account that  $\overline{S}'_{0,\pm}(\bar{x}) = (S'_{0,\pm}(x))^*$ . Notice that the exponent in the r.h.s. of (3.19) does not receive the  $\mathcal{O}(\eta^0)$ -correction, since  $S'_1(x)$  is single-valued on the  $x$ -plane. Since the l.h.s. of (3.19) does not depend on  $j$ , one gets from (3.19) the set of consistency conditions

$$\exp\left(\frac{2i}{\eta} \operatorname{Re} \int_{\sigma_k}^{\sigma_j} dx [S'_{0,-}(x) - S'_{0,+}(x)] + \mathcal{O}(\eta)\right) = 1. \quad (3.20)$$

The quantization conditions (3.19) and (3.20) can be expressed in a concise form in terms of the contour integrals on the Riemann surface  $\Gamma_N$ , Eq. (1.10). We recall that the two branches  $S'_{0,\pm}(x)$  define the dipole differential  $dx S'_0(x)$  on  $\Gamma_N$ . This allows one to rewrite (3.19) as

$$\frac{c_+(0)}{c_-(0)} = \exp\left(-\frac{2i}{\eta} \operatorname{Re} \int_{P_0^-}^{P_0^+} dx S'_0(x) + \mathcal{O}(\eta)\right) \equiv e^{-2i\Theta}, \quad (3.21)$$

with  $\Theta$  some (real) constant introduced for later convenience. Here integration goes over an arbitrary path on  $\Gamma_N$ , which starts at the point  $P_0^-$  located above  $x = 0$  on the lower sheet and ends at the point  $P_0^+$  above  $x = 0$  on the upper sheet.

Let us define the canonical basis of oriented cycles on  $\Gamma_N$  as shown in Figure 1. The contour integral in Eq. (3.21) can be uniquely decomposed over this basis as

$$\int_{P_0^-}^{P_0^+} = \int_{\gamma_{P_0^- P_0^+}} + \sum_{j=1}^{N-2} k_j \oint_{\alpha_j} + \sum_{j=1}^{N-2} m_j \oint_{\beta_j}, \quad (3.22)$$

with  $k_j$  and  $m_j$  arbitrary integer. Here, the path  $\gamma_{P_0^- P_0^+}$  goes from the point  $P_0^-$  on the lower sheet to the point  $P_0^+$  on the upper sheet and it does not cross the canonical cycles (see Figure 1). The l.h.s. of (3.21) should not depend on the choice of the integration path, or equivalently on integers  $k_j$  and  $m_j$  in Eq. (3.22). This leads to

$$\operatorname{Re} \oint_{\alpha_k} dx S'_0(x)/\eta = \pi \ell_{2k-1}, \quad \operatorname{Re} \oint_{\beta_k} dx S'_0(x)/\eta = \pi \ell_{2k}, \quad (3.23)$$

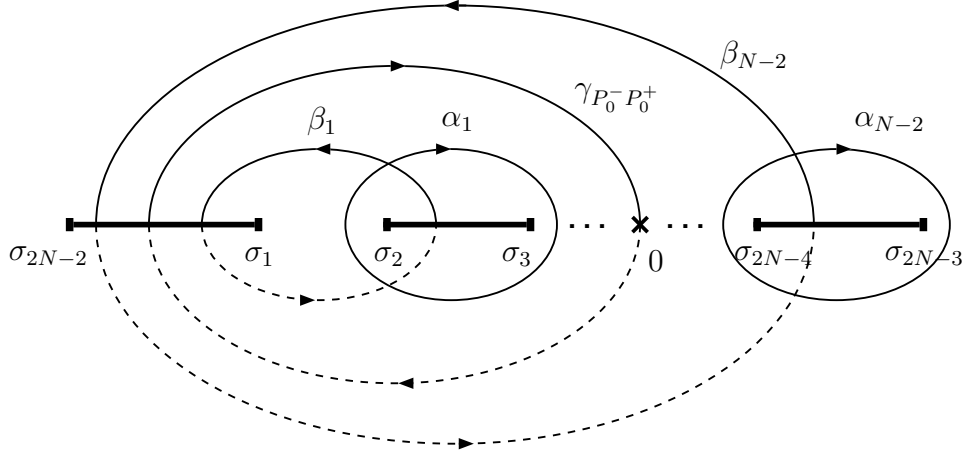


Figure 1: The canonical basis of oriented  $\alpha$ - and  $\beta$ -cycles on the Riemann surface  $\Gamma_N$ . The dotted line represents the part of the  $\beta$ -cycles on the lower sheet. The cross denotes a projection of the points  $P_0^\pm$  onto the complex plane. The path  $\gamma_{P_0^- P_0^+}$  goes from the point  $P_0^-$  on the lower sheet to the point  $P_0^+$  on the upper sheet.

with  $S_0(x)$  defined in (3.6),  $k = 1, \dots, N-2$  and  $\ell = (\ell_1, \dots, \ell_{2N-4})$  being integer. These relations establish the WKB quantization conditions for the integrals of motion of the model. In addition, one finds from (3.22) and (3.21)

$$\text{Re} \int_{\gamma_{P_0^- P_0^+}} dx S'_0(x)/\eta = \Theta. \quad (3.24)$$

The following comments are in order.

Eqs. (3.23) and (3.24) are valid up to corrections suppressed by a *second* power of  $\eta$ . One can show that this feature is rather general and the WKB expansion in the l.h.s. of (3.23) and (3.24) goes over *even* powers of  $\eta$ .

We recall that, by the definition,  $\eta$  is a small auxiliary parameter which was introduced in (3.1) in order to formulate the WKB expansion. The spectrum of the model should not depend on  $\eta$ . Indeed, one verifies using (3.6) and (3.1), that the l.h.s. of (3.23) and (3.24), as well as  $q_n = \widehat{q}_n/\eta^n$ , stay invariant under the scaling transformation  $x \rightarrow \lambda x$ ,  $\eta \rightarrow \lambda \eta$  and  $\widehat{q}_n \rightarrow \widehat{q}_n \lambda^n$ . Therefore we may choose  $\eta$  in Eqs. (3.23) and (3.24) to our best convenience, say  $\eta = 1$ , but keep in mind, of course, that the WKB approximation is valid for large values of the charges  $q_n$ . In this way, one arrives at the quantization conditions (1.13). Their solutions have the form (1.4) and are parameterized by the set of integers  $\ell = (\ell_1, \dots, \ell_{2(N-2)})$ .

As we will show in Section 4, the phase  $\Theta$  in the r.h.s. of (3.24) is closely related to the quasimomentum  $\theta_N$  corresponding to the eigenstate (3.15). Evaluating the contour integral in the l.h.s. of (3.24) and replacing the charges  $q_n$  by their quantized values, Eq. (1.4), one can obtain from (3.24) the dependence of the quasimomentum on integers  $\ell$ .

A novel feature of the quantization conditions (3.23) compared to the conventional WKB approach [16, 18, 25] is that they involve *both*  $\alpha$ - and  $\beta$ -periods on the Riemann surface  $\Gamma_N$ . We remind that the Hamiltonian of the  $SL(2, \mathbb{C})$  magnet is given by the sum of two one-dimensional mutually commuting Hamiltonians “living” on the  $z$ - and  $\bar{z}$ -lines. If we  $z$  and  $\bar{z}$  have been

real coordinates, each of these Hamiltonian would have defined quantum  $SL(2, \mathbb{R})$  Heisenberg magnet. The WKB quantization conditions for this magnet look as follows [17, 20, 21]

$$SL(2, \mathbb{R}) : \quad \oint_{\alpha_k} dx S'_0(x)/\eta = 2\pi(\ell_k + 1/2), \quad (3.25)$$

with the “action” differential,  $dx S'_0(x)$ , and the Riemann surface,  $\Gamma_N$ , the same as in the  $SL(2, \mathbb{C})$  case, Eqs. (3.6) and (1.10), respectively. A crucial difference between the  $SL(2, \mathbb{C})$  and  $SL(2, \mathbb{R})$  magnets is that the integrals of motion,  $q_n$ , and the separated variables,  $x$  and  $p_x$ , take real values in the latter case. As a consequence, the classical motion in the separated  $SL(2, \mathbb{R})$  coordinates is restricted to the intervals on the real  $x$ -axis on which  $t_N^2(x) - 4x^{2N} \geq 0$  (see Eq. (3.5)). The integration in (3.25) goes along the cycles (real slices of  $\Gamma_N$ ) encircling these intervals on the complex  $x$ -plane. In the  $SL(2, \mathbb{C})$  case, the classical trajectories wrap arbitrarily around  $\Gamma_N$  and, as a consequence, the quantization conditions (3.23) involve also  $\beta$ -cycles which correspond, from point of view of the  $SL(2, \mathbb{R})$  magnet, to classically forbidden zones.

We shall solve the quantization conditions (3.23) in Section 5.

## 4. Quasiclassical spectrum

The WKB analysis performed in the previous Section allowed us to formulate the quantization conditions for the integrals of motion, Eqs. (3.23), and construct the WKB expression for the wave function in the separated coordinates, Eq. (3.15). Let us extend our analysis and evaluate the physical observables of the model – the energy,  $E_N$ , and the quasimomentum,  $\theta_N$ .

Our starting point will be the expressions for  $E_N$  and  $\theta_N$  obtained in Ref. [5, 10] within the method of the Baxter  $\mathbb{Q}$ -operator (see Eqs. (4.6) and (4.7) below). They are formulated in terms of the eigenvalue of the Baxter  $\mathbb{Q}$ -operator,  $Q(u, \bar{u})$ , which is a function of two complex spectral parameters,  $u$  and  $\bar{u}$ , such that  $i(u - \bar{u}) = n$  with  $n$  arbitrary integer. The wave function in the SoV representation,  $Q(x, \bar{x})$  (see Eq. (2.9)), coincides with this function for  $u = \nu - in/2$  and  $\bar{u} = \nu - in/2$  with  $\nu$  real. In this way,  $Q(u, \bar{u})$  can be considered as an analytical continuation of the wave function from the real axis to the whole complex  $\nu$ -plane.

The energy spectrum of the quantum  $SL(2, \mathbb{C})$  magnet is related to the behaviour of the function  $Q(u, \bar{u})$  around two special points on the complex  $\nu$ -plane corresponding to  $u = \pm is$  and  $\bar{u} = \pm i\bar{s}$  with  $(s, \bar{s})$  being a single-particle  $SL(2, \mathbb{C})$  spin, Eq. (1.1). We notice that this behaviour can not be deduced from the obtained WKB expression for the  $Q$ -function (3.15) since the latter is valid only for large  $u$  and  $\bar{u}$ . In this Section, we shall construct an asymptotic expression for  $Q(u, \bar{u})$ , valid for large charges  $q_n$  and  $u, \bar{u} = \text{fixed}$ , and use it to calculate the quasiclassical energy spectrum.

### 4.1. Baxter $Q$ -blocks

To begin with, we summarize, following [10], the main properties of the eigenvalues of the Baxter  $\mathbb{Q}$ -operator,  $Q(u, \bar{u})$ . The function  $Q(u, \bar{u})$  can be decomposed into a bilinear combination of chiral blocks

$$Q(u, \bar{u}) = e^{-i\delta} Q_0(u)\bar{Q}_0(\bar{u}) - e^{i\delta} Q_1(u)\bar{Q}_1(\bar{u}), \quad (4.1)$$

with  $\delta$  arbitrary complex. The blocks  $Q_0(u)$  and  $Q_1(u)$  satisfy the chiral Baxter equation (2.11) for arbitrary complex  $u$  and fulfil the Wronskian condition

$$Q_0(u+i)Q_1(u) - Q_0(u)Q_1(u+i) = \frac{\Gamma^N(iu-s)}{\Gamma^N(iu+s)}. \quad (4.2)$$

Similar blocks in the antiholomorphic sector,  $\overline{Q}_0(\bar{u})$  and  $\overline{Q}_1(\bar{u})$ , are defined as

$$Q_1(u) = \frac{\Gamma^N(1-s+iu)}{\Gamma^N(s+iu)}(\overline{Q}_0(u^*))^*, \quad \overline{Q}_1(\bar{u}) = \frac{\Gamma^N(1-\bar{s}-i\bar{u})}{\Gamma^N(\bar{s}-i\bar{u})}(Q_0(\bar{u}^*))^*. \quad (4.3)$$

The  $Q$ -blocks are meromorphic functions on the complex plane. Their analytical properties can be summarized as

$$Q_0(u) = \Gamma^{N-1}(1-s+iu)f(u), \quad \overline{Q}_0(\bar{u}) = \Gamma^{N-1}(1-\bar{s}-i\bar{u})\bar{f}(\bar{u}), \quad (4.4)$$

where  $f(u)$  and  $\bar{f}(\bar{u})$  are entire functions. As was already mentioned, at  $u = x$  and  $\bar{u} = x^*$  with  $x$  given by (2.10),  $Q(u, \bar{u})$  defines the wave function in the separated coordinates, Eq. (2.9). The constant  $\delta$  in (4.1) is fixed by the requirement that  $Q(\nu - in/2, \nu + in/2)$  should not have poles for real  $\nu$ . The same condition can be expressed as [10]

$$Q(i(1-s) + \epsilon, -i\bar{s} + \epsilon) = \mathcal{O}(\epsilon^0), \quad Q(-is + \epsilon, i(1-\bar{s}) + \epsilon) = \mathcal{O}(\epsilon^0), \quad (4.5)$$

for  $\epsilon \rightarrow 0$  and  $\bar{s} = 1 - s^*$ .

The energy and the quasimomentum of the model are expressed in terms of the  $Q$ -blocks as

$$E_N = -2 \operatorname{Im} (\ln Q_0(is))' + 2 \operatorname{Im} (\ln \overline{Q}_0(-i\bar{s}))' + \varepsilon_N, \quad (4.6)$$

$$\theta_N = i \ln \frac{Q_0(is) \overline{Q}_0(i\bar{s})}{Q_0(-is) \overline{Q}_0(-i\bar{s})}. \quad (4.7)$$

where  $\varepsilon_N = 2N \operatorname{Re} [\psi(2s) + \psi(2-2s) - 2\psi(1)]$ .

Thus, the problem of calculating the energy spectrum of the model is reduced to finding the blocks  $Q_0(u)$  and  $\overline{Q}_0(\bar{u})$ . Their exact expressions were obtained in [10]. In this Section we shall obtain asymptotic expressions for the blocks  $Q_0(u)$  and  $\overline{Q}_0(\bar{u})$  valid for large charges  $q_n$  and fixed spectral parameters  $u$  and  $\bar{u}$ .

## 4.2. Asymptotic solutions to the Baxter equation

Let us rewrite the Baxter equation (2.11) for the block  $Q_0(u)$  as

$$(u+is)^N q(u) + (u-is)^N \frac{1}{q(u-i)} = t_N(u), \quad (4.8)$$

where the notation was introduced for  $q(u) = Q_0(u+i)/Q_0(u)$ . We notice that for large charges  $q_n$  and fixed  $u$  the polynomial  $t_N(u)$ , defined in (1.10), takes large values  $|t_N(u)| \gg 1$ . This suggests to expand the solutions to (4.8) in inverse powers of  $t_N(u)$ . Assuming that one of the terms in the l.h.s. of (4.8) is much smaller than another one, we obtain two solutions

$$q_+(u) = \frac{t_N(u)}{(u+is)^N} + \dots, \quad q_-(u-i) = \frac{(u-is)^N}{t_N(u)} + \dots \quad (4.9)$$



Here, ellipses denote subleading corrections controlled by the parameter

$$\left| \frac{(u \pm is)^N (u \pm i(1-s))^N}{t_N(u) t_N(u \pm i)} \right| \ll 1. \quad (4.10)$$

Eq. (4.9) gives rise to two linear independent asymptotic solutions for the block  $Q_0(u)$ . The general expression for  $Q_0(u)$  with the prescribed analytical properties (4.4) takes the form

$$Q_0^{(\text{as})}(u) = \frac{\Gamma^{N-1}(1-s+iu)}{\Gamma(s-iu)} \varphi_+(u) + \frac{1}{\Gamma^N(s+iu)} \varphi_-(u), \quad (4.11)$$

where  $\varphi_{\pm}(u)$  are *entire* functions satisfying the functional equations

$$\frac{\varphi_+(u+i)}{\varphi_+(u)} = -i^N t_N(u), \quad \frac{\varphi_-(u-i)}{\varphi_-(u)} = i^N t_N(u). \quad (4.12)$$

It is important to realize that the particular form of the ratio of the  $\Gamma$ -functions in the r.h.s. of (4.11) is uniquely fixed by analytical properties of the block  $Q_0(u)$ , Eq. (4.4). If any  $\Gamma$ -function in (4.11) was substituted as  $\Gamma(x) \rightarrow 1/\Gamma(1-x)$ , one would obtain another solution to the Baxter equation (4.8) (up to corrections suppressed by the factor (4.10)) but its pole structure would be different from (4.4).

The  $\bar{Q}$ -block in the antiholomorphic sector is given by similar expression

$$\bar{Q}_0^{(\text{as})}(\bar{u}) = \frac{\Gamma^{N-1}(1-\bar{s}-i\bar{u})}{\Gamma(\bar{s}+i\bar{u})} \bar{\varphi}_+(\bar{u}) + \frac{1}{\Gamma^N(\bar{s}-i\bar{u})} \bar{\varphi}_-(\bar{u}), \quad (4.13)$$

with  $\bar{\varphi}_{\pm}(\bar{u})$  entire functions satisfying the relations

$$\frac{\bar{\varphi}_+(\bar{u}-i)}{\bar{\varphi}_+(\bar{u})} = -(-i)^N \bar{t}_N(\bar{u}), \quad \frac{\bar{\varphi}_-(\bar{u}+i)}{\bar{\varphi}_-(\bar{u})} = (-i)^N \bar{t}_N(\bar{u}). \quad (4.14)$$

Here  $\bar{t}_N(\bar{u})$  is given by (1.10) with the charges  $q_n$  replaced by their antiholomorphic counterparts  $\bar{q}_n = q_n^*$ , so that  $\bar{t}_N(\bar{u}) = t_N(\bar{u}^*)^*$ . Substituting (4.11) and (4.13) into (4.3) we obtain

$$\begin{aligned} Q_1^{(\text{as})}(u) &= \frac{\sin(\pi(s+iu))}{\pi} \Gamma^N(1-s+iu) (\bar{\varphi}_+(u^*))^* + \frac{1}{\Gamma^N(s+iu)} (\bar{\varphi}_-(u^*))^*, \\ \bar{Q}_1^{(\text{as})}(\bar{u}) &= \frac{\sin(\pi(\bar{s}-i\bar{u}))}{\pi} \Gamma^N(1-\bar{s}-i\bar{u}) (\varphi_+(\bar{u}^*))^* + \frac{1}{\Gamma^N(\bar{s}-i\bar{u})} (\varphi_-(\bar{u}^*))^*. \end{aligned} \quad (4.15)$$

To solve (4.12) and (4.14) one factorizes the polynomial  $t_N(u)$ , Eq. (1.10), as

$$t_N(u) = 2u^N + q_2 u^{N-2} + \dots + q_N = 2 \prod_{k=1}^N (u - \lambda_k). \quad (4.16)$$

For arbitrary, large  $q_n \sim 1/\eta^n$  its roots take, in general, large complex values,  $\lambda_n \sim 1/\eta$  and satisfy the sum rules

$$\sum_k \lambda_k = 0, \quad \sum_{k>n} \lambda_k \lambda_n = q_2/2, \quad \dots, \quad \prod_k \lambda_k = (-1)^N q_N/2. \quad (4.17)$$

Substituting (4.16) into (4.12) one can write a particular solution for  $\varphi_+(u)$  in the form

$$\varphi_+^{(\text{naive})}(u) \sim e^{\pm\pi u} 2^{-iu} \prod_{k=1}^N \Gamma(i\lambda_k - iu). \quad (4.18)$$

As before, substituting  $\Gamma(x) \rightarrow 1/\Gamma(1-x)$  in the r.h.s. of (4.18) one can get yet another solution to (4.12). To fix this ambiguity we require that  $\varphi_+(u)$  has to be an entire function of  $u$  in the region  $u \sim \eta^0$ . Therefore, the product of the  $\Gamma$ -function in the r.h.s. of (4.18) should not generate poles for  $u \sim \eta^0$ . Decomposing  $\lambda_k$  into real and imaginary parts,  $\Gamma(i\lambda_k - iu) = \Gamma(i \operatorname{Re} \lambda_k - \operatorname{Im} \lambda_k - iu)$ , one finds that in spite of the fact that  $\lambda_k \sim 1/\eta$ , the roots with  $\operatorname{Im} \lambda_k \sim 1/\eta$  and  $\operatorname{Re} \lambda_k \sim \eta^0$  generate the sequence of poles located at  $iu = i \operatorname{Re} \lambda_k - [\operatorname{Im} \lambda_k] + n \sim \eta^0$  with  $n$  nonnegative integer and [...] denoting the entire part.

This suggests to separate all roots in (4.18) into two sets according to  $\operatorname{Im} \lambda_k \geq 0$  and  $\operatorname{Im} \lambda_k < 0$  and look for the solutions to (4.12) in the form

$$\varphi_+(u) = a_+(u) \widehat{\varphi}_+(u), \quad \varphi_-(u) = a_-(u) \widehat{\varphi}_-(u), \quad (4.19)$$

where the notation was introduced for the basis functions

$$\begin{aligned} \widehat{\varphi}_+(u) &= 2^{-iu} \prod_{\operatorname{Im} \lambda_k < 0} \Gamma(i\lambda_k - iu) \prod_{\operatorname{Im} \lambda_k \geq 0} \frac{1}{\Gamma(1 - i\lambda_k + iu)}, \\ \widehat{\varphi}_-(u) &= 2^{iu} \prod_{\operatorname{Im} \lambda_k \geq 0} \Gamma(-i\lambda_k + iu) \prod_{\operatorname{Im} \lambda_k < 0} \frac{1}{\Gamma(1 + i\lambda_k - iu)}. \end{aligned} \quad (4.20)$$

In these expressions, the roots with  $\operatorname{Re} \lambda_k \sim \eta^0$  do not generate spurious poles. In similar manner, the solutions to the antiholomorphic relations in (4.14) are given by

$$\overline{\varphi}_+(\bar{u}) = \overline{a}_+(\bar{u}) (\widehat{\varphi}_+(\bar{u}^*))^*, \quad \overline{\varphi}_-(\bar{u}) = \overline{a}_-(\bar{u}) (\widehat{\varphi}_-(\bar{u}^*))^*. \quad (4.21)$$

Substituting (4.19) and (4.21) into (4.12) and (4.14), respectively, we find that the functions  $a_{\pm}(u)$  and  $\overline{a}_{\pm}(\bar{u})$  are entire (anti)periodic functions satisfying the functional relations

$$a_{\pm}(u \pm i) = \mp(-1)^{N_-} a_{\pm}(u), \quad \overline{a}_{\pm}(\bar{u} \mp i) = \mp(-1)^{N_-} \overline{a}_{\pm}(\bar{u}). \quad (4.22)$$

Here,  $N_-$  denotes the number of roots (4.17) with  $\operatorname{Im} \lambda_k$  negative

$$N_- = \sum_{\operatorname{Im} \lambda_k < 0} 1, \quad N_+ = \sum_{\operatorname{Im} \lambda_k \geq 0} 1, \quad N_+ + N_- = N. \quad (4.23)$$

Inserting (4.19) and (4.21) into (4.11) and (4.13), one obtains asymptotic expressions for the Baxter blocks  $Q_0(u)$  and  $\overline{Q}_0(\bar{u})$ . They depend however on four yet undefined functions  $a_{\pm}(u)$  and  $\overline{a}_{\pm}(\bar{u})$ . Additional constraints on these functions are derived in Appendix A (see Eq. (A.14)). They come from two different sources. First, one has to ensure that the obtained expressions for the blocks verify the Wronskian condition (4.2). Second, for  $u = \nu - in/2$  and  $\bar{u} = u^*$  (with  $\nu$  real and  $n$  integer) the function  $Q(u, \bar{u})$  coincides with the wave function in the separated coordinates. Substituting the asymptotic expressions for the blocks into (4.1) and continuing the resulting expression to the region of large  $u$ , one should be able to match it into analogous expression for the WKB wave function (3.15). The matching procedure is performed in Appendix A.

### 4.3. Energy spectrum

According to (4.6) and (4.7), the energy and quasimomentum are related to the behaviour of the blocks  $Q_0(u)$  and  $\overline{Q}_0(\bar{u})$  around the points  $u = \pm is$  and  $\bar{u} = \pm i\bar{s}$ . Substituting the obtained asymptotic expressions for the blocks, Eqs. (4.11) and (4.13), into the expression for the quasimomentum, Eq. (4.7), one finds after some calculation (see Appendix B for detail)

$$\theta_N = -2\Theta = -2 \operatorname{Re} \int_{\gamma_{P_0^- P_0^+}} dx S'_0(x) = -2 \operatorname{Re} \int_{P_0^-}^{P_0^+} dx S'_0(x) \pmod{2\pi}. \quad (4.24)$$

Here in the second relation we replaced the phase  $\Theta$  by its expression (3.24) and put  $\eta = 1$ . The contour integral in the r.h.s. of (4.24) depends on the integrals of motion  $q_n$ . Since the possible values of the quasimomentum are given by  $\theta_N = 2\pi\ell/N$  with  $\ell$  being integer, one should expect that for  $q_n$  satisfying the quantization conditions (3.23) the integral takes the same quantized values. Indeed, we demonstrate this property in Appendix B by an explicit calculation of (4.24).

The calculation of the energy (4.6) goes along the same lines (see Appendix B). It leads to the following asymptotic expression for the energy

$$\begin{aligned} E_N^{(\text{as})} &= 4 \ln 2 + 2 \operatorname{Re} \sum_{\operatorname{Im} \lambda_k \geq 0} \left[ \psi(1 - s - i\lambda_k) + \psi(s - i\lambda_k) - 2\psi(1) \right] \\ &\quad + 2 \operatorname{Re} \sum_{\operatorname{Im} \lambda_k < 0} \left[ \psi(1 - s + i\lambda_k) + \psi(s + i\lambda_k) - 2\psi(1) \right]. \end{aligned} \quad (4.25)$$

Here, the sum goes over the (complex) roots of the polynomial  $t_N(u)$ , Eqs. (4.16) and (4.17). By the definition, their total number equals the number of particles,  $N$ , and their values depend on the integrals of motion  $q_n$ . Since the latter are quantized according to (1.4), the relation (4.25) establishes the dependence of the energy on the total set of quantum numbers, Eq. (1.4).

The obtained expression for the energy (4.25) is symmetric under  $s \rightarrow 1 - s$ . This is in agreement with the fact that the  $SL(2, \mathbb{C})$  representations of the spin  $s$  and  $1 - s$  are unitary equivalent and, as a consequence, the corresponding spin magnets should have the same energy spectrum.

According to (4.25), the roots with  $\operatorname{Im} \lambda_k > 0$  and  $\operatorname{Im} \lambda_k < 0$  provide different contribution to the energy. To elucidate this property let us examine (4.25) for the  $SL(2, \mathbb{C})$  spin  $s = 0$

$$E_N^{(\text{as})} \Big|_{s=0} = 4 \ln 2 + 2 \operatorname{Re} \sum_{k=0}^N \left[ \psi(1 + i \operatorname{Re} \lambda_k + |\operatorname{Im} \lambda_k|) + \psi(i \operatorname{Re} \lambda_k + |\operatorname{Im} \lambda_k|) - 2\psi(1) \right], \quad (4.26)$$

where  $\lambda_k$  are roots of the polynomial  $t_N(u)$ , Eq. (4.16). We recall that the Euler  $\psi$ -function has poles at nonpositive integer values of its argument. In the r.h.s. of (4.26) these poles are never approached for arbitrary charges  $q_n$  provided that  $q_N \neq 0$ .

Let us compare the asymptotic expression for the energy, Eq. (4.26), with the results of the exact calculation [9, 10]. For the sake of simplicity, we choose the total Lorentz spin of the model to be  $n_h = 0$ , so that the total  $SL(2, \mathbb{C})$  spin (1.5) equals  $h = 1/2 + i\nu_h$ , and examine the dependence of the energy  $E_N^{(\text{as})} \Big|_{s=0}$  on real  $\nu_h$  along a few lowest lying trajectories at  $N = 3$  and  $N = 4$ . Applying (4.26) and (4.16), we substitute  $q_2 = 1/4 + \nu_h^2$  and replace the charges  $q_3, \dots, q_N$  by their exact values found in Ref. [9, 10]. Comparison with the exact expression for

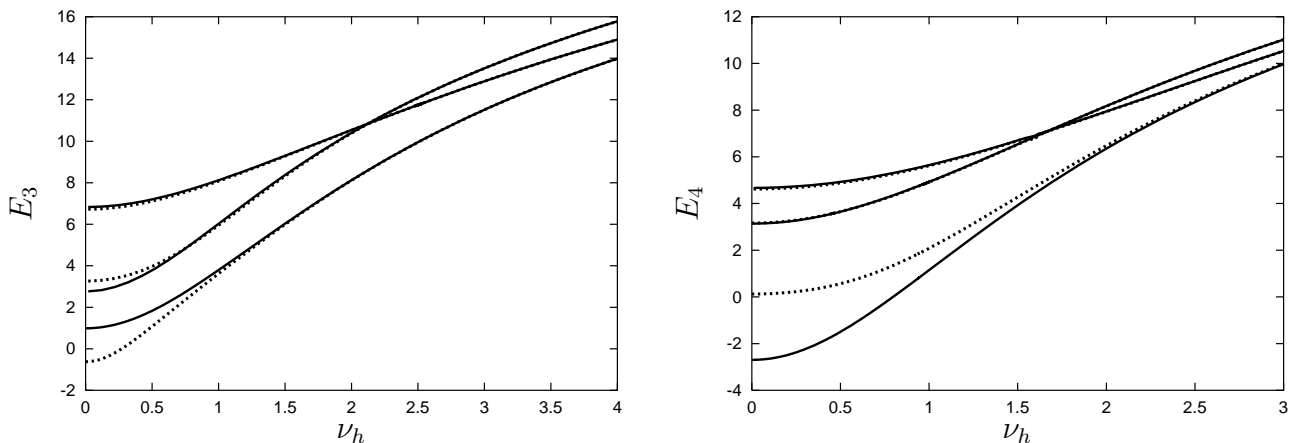


Figure 2: Dependence of the energy  $E_N^{(s=0)}$  on the total spin  $h = 1/2 + i\nu_h$  for the three lowest eigenstates at  $N = 3$  (left panel) and  $N = 4$  (right panel). The solid lines denote the exact energy from Refs. [9, 10], the dotted lines describe the asymptotic expression (4.26) calculated for the exact charges  $q_3$  and  $q_4$ .

the energy is shown in Figure 2. We recall that Eqs. (4.25) and (4.26) were obtained to the leading order of the WKB expansion under assumption that the “energies”  $q_2, \dots, q_N$  are large. Therefore, it is not surprising that the quasiclassical expression for the ground state trajectory agrees with the exact energy only for  $\nu_h > 1$ . At the same time, for the excited trajectories the agreement is rather remarkable (especially at  $N = 4$ ) even for smaller  $\nu_h$ .

In Section 3.2 we already drew the analogy between the quantization conditions for the  $SL(2, \mathbb{C})$  and  $SL(2, \mathbb{R})$  magnets. It can be further extended to the asymptotic expressions for the energy. For the  $SL(2, \mathbb{R})$  magnet the corresponding expression looks like [19, 20, 21]

$$SL(2, \mathbb{R}) : \quad E_N^{(\text{as})} \Big|_{s=0} = 2 \ln 2 + \text{Re} \sum_{k=0}^N \left[ \psi(1 + i\lambda_k) + \psi(i\lambda_k) - 2\psi(1) \right]. \quad (4.27)$$

Here, in distinction with the  $SL(2, \mathbb{C})$  case, the roots  $\lambda_k$  take strictly real values. Similarity between Eqs. (4.26) and (4.27) suggests that there should exist a relation between the energy spectrum of the  $SL(2, \mathbb{C})$  and  $SL(2, \mathbb{R})$  magnets. Indeed, it can be shown that the latter can be obtained from the former by *analytical continuation* in the total spin of the system, Eq. (1.5), from real  $\nu_h$  to pure imaginary  $\nu_h$ .

## 5. Solving the quantization conditions

In previous Section we derived the WKB quantization conditions for the integrals of motions of the  $SL(2, \mathbb{C})$  magnet, Eq. (3.23), and obtained the expressions for the energy spectrum, Eqs. (4.25) and (4.24). In this Section, we shall solve the quantization conditions (3.23) and reconstruct a fine structure of the spectrum.

The general solutions to (3.23) have the form (1.4). The spectrum of quantized charges  $q_n$  is parameterized by the set of integers  $\ell = (\ell_1, \dots, \ell_{2N-4})$  entering the r.h.s. of (3.23), as well as by continuous real  $\nu_h$  and integer  $n_h$  defining the total  $SL(2, \mathbb{C})$  spin of the magnet, Eq. (1.5). We recall that the quantization conditions (3.23) involve the periods of the “action” differential

over the canonical basis of oriented cycles,  $\boldsymbol{\alpha} = (\alpha_1, \dots, \alpha_{N-2})$  and  $\boldsymbol{\beta} = (\beta_1, \dots, \beta_{N-2})$ , on the Riemann surface  $\Gamma_N$  of genus  $g = N - 2$ . The definition of this basis on  $\Gamma_N$  is ambiguous [22]

$$\boldsymbol{\alpha} \rightarrow \boldsymbol{\alpha}' = a \cdot \boldsymbol{\alpha} + b \cdot \boldsymbol{\beta}, \quad \boldsymbol{\beta} \rightarrow \boldsymbol{\beta}' = c \cdot \boldsymbol{\alpha} + d \cdot \boldsymbol{\beta}, \quad (5.1)$$

where  $a, b, c$  and  $d$  are  $(N - 2) \times (N - 2)$  matrices with integer entries such that

$$Z = \begin{pmatrix} a & b \\ c & d \end{pmatrix}, \quad \det Z = 1, \quad Z^t \begin{pmatrix} 0 & \mathbf{1} \\ -\mathbf{1} & 0 \end{pmatrix} Z = \begin{pmatrix} 0 & \mathbf{1} \\ -\mathbf{1} & 0 \end{pmatrix}, \quad (5.2)$$

so that  $Z \in \text{Sp}(N-2, \mathbb{Z})$ . Notice that  $Z \in \text{SL}(2, \mathbb{Z})$  for  $N = 3$ . The spectrum of the model should not depend on the choice of the basis. Indeed, the quantization conditions (3.23) stay invariant under the  $\text{Sp}(N - 2, \mathbb{Z})$  transformation (5.1) provided that the integers  $\boldsymbol{\ell}_{\text{odd}} = (\ell_1, \dots, \ell_{2N-5})$  and  $\boldsymbol{\ell}_{\text{even}} = (\ell_2, \dots, \ell_{2N-4})$  are transformed in the same way

$$\boldsymbol{\ell}_{\text{odd}} \rightarrow \boldsymbol{\ell}'_{\text{odd}} = a \cdot \boldsymbol{\ell}_{\text{odd}} + b \cdot \boldsymbol{\ell}_{\text{even}}, \quad \boldsymbol{\ell}_{\text{even}} \rightarrow \boldsymbol{\ell}'_{\text{even}} = c \cdot \boldsymbol{\ell}_{\text{odd}} + d \cdot \boldsymbol{\ell}_{\text{even}}. \quad (5.3)$$

This relation establishes the correspondence between two different solutions to the quantization conditions labelled by the sets of integers  $\boldsymbol{\ell}$  and  $\boldsymbol{\ell}'$ .

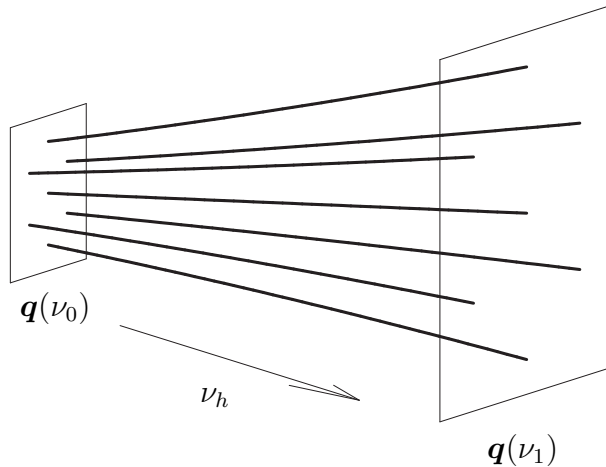


Figure 3: Flow of the quantized values of the integrals of motion  $\mathbf{q} = (q_2, \dots, q_N)$  with  $\nu_h$ .

As was shown in Ref. [10], quantized values of the charges,  $q_n(\nu; n_h, \boldsymbol{\ell})$ , form the family of one-dimensional nonintersecting trajectories on the  $(N - 1)$ -dimensional space of  $\mathbf{q} = (q_2, \dots, q_N)$  (see Figure 3). Each member of the family is labelled by integers  $n_h$  and  $\boldsymbol{\ell}$ , while the “proper time” along the trajectory is defined by  $\nu_h$ . The quasiclassical approach allows us to reconstruct the trajectories in two different limits: (i)  $\boldsymbol{\ell} = \text{large}$  and  $\nu_h = \text{fixed}$ ; (ii)  $\boldsymbol{\ell} = \text{fixed}$  and  $\nu_h = \text{large}$ . In the both cases, the integrals of motion take large values, so that the quasiclassical approach is applicable. In the first case, we shall find the points on the  $\mathbf{q}$ -space, at which the trajectories pierce the hyperplane  $\nu_h = \text{fixed}$ , and demonstrate that their positions define a lattice-like structure on the moduli space (see Figure 3). In the second case, we shall describe the flow of these points with  $\nu_h$  along the trajectories.

## 5.1. Lattice structure

Before we proceed with evaluating the contour integrals entering (3.23), let us rewrite the quantization conditions in a slightly different form. From the expression for the quasimomentum (4.24) one gets

$$\theta_N = 2 \operatorname{Re} \int_{\gamma(\sigma_k)} dx S'_0(x) = \frac{2\pi}{N} \ell \pmod{2\pi}. \quad (5.4)$$

Here the integration contour  $\gamma(\sigma_k)$  goes from the point  $P_0^+$  above  $x = 0$  on the upper sheet of  $\Gamma_N$  to the branching point  $\sigma_k$ , encircles it and goes to the point  $P_0^-$  on the lower sheet of  $\Gamma_N$ . The quasimomentum  $\theta_N$  describes the transformation properties of the eigenfunction under the cyclic permutations of  $N$  particles,  $\Psi(\vec{z}_2, \dots, \vec{z}_N, \vec{z}_1) = e^{i\theta_N} \Psi(\vec{z}_1, \dots, \vec{z}_{N-1}, \vec{z}_N)$ . Its value satisfy  $\exp(iN\theta_N) = 1$ , so that  $\ell$  is integer in the r.h.s. of (5.4),  $0 \leq \ell \leq N - 1$ . One concludes from (5.4) that

$$\frac{1}{\pi} \operatorname{Re} \int_{\gamma(\sigma_k)} dx S'_0(x) = \frac{\ell}{N} + n_k, \quad (5.5)$$

with  $k = 1, \dots, 2(N - 1)$  and  $n_k$  integer. Remarkably enough, the quantization conditions (3.23) are equivalent to the system of equations (5.5). To see this, one rewrites the  $\alpha$ - and  $\beta$ -periods of the “action” differential as (see Figure 1)  $\oint_{\alpha_k} = \int_{\gamma(\sigma_{2k+1})} - \int_{\gamma(\sigma_{2k})}$  and  $\oint_{\beta_k} = \int_{\gamma(\sigma_1)} - \int_{\gamma(\sigma_{2k})}$ . Substituting these relations into (3.23), one finds that the quantization conditions (3.23) can be expressed as a linear combination of integrals entering the l.h.s. of (5.5). In this way, one establishes the correspondence between two sets of integers

$$n_{2k+1} - n_{2k} = \ell_{2k-1}, \quad n_1 - n_{2k} = \ell_{2k}. \quad (5.6)$$

Eq. (5.5) involves a rather complicated contour integral on the hyperelliptic curve  $\Gamma_N$ . Although it is straightforward to calculate it numerically for a given set of the integrals of motion  $\mathbf{q}$ , this does not allow us to understand a general structure of solutions to (5.5).

To this end, let us examine the quantization conditions (5.5) in the limit

$$q_2 = \mathcal{O}(\epsilon^0), \quad q_n = \mathcal{O}(\epsilon^{-(n-2)/2}), \quad q_N = \mathcal{O}(\epsilon^{-N/2}) \quad (5.7)$$

with  $\epsilon \ll 1$  and  $n = 3, \dots, N - 1$ . This hierarchy corresponds to large  $q_3, \dots, q_N$  and fixed  $q_2$ . The main advantage of (5.7) is that the spectral curve  $\Gamma_N$ , Eq. (1.10), simplifies significantly and integration in (3.23) can be performed analytically. Indeed, after the scaling transformation  $x \rightarrow (q_N/4)^{1/N} x$ ,  $y \rightarrow q_N y$  the spectral curve (1.10) takes the form

$$\Gamma_N^{(\text{as})} : \quad y^2 = (x^N + 1 + p_{N-2}(x))(1 + p_{N-2}(x)) + \mathcal{O}(\epsilon^2), \quad (5.8)$$

where

$$p_{N-2}(x) = \sum_{n=2}^{N-1} u_n x^{N-n}, \quad u_n = \frac{q_n}{4} \left( \frac{q_N}{4} \right)^{-n/N} = \mathcal{O}(\epsilon) \quad (5.9)$$

Comparing (5.8) with (1.10) and (3.7), we find that  $N$  branching points of the curve  $\Gamma_N^{(\text{as})}$  are located at the vertices of the  $N$ -polygon, whereas the remaining  $N - 2$  points are located far from the origin on the complex plane

$$\sigma_m^{(\text{as})} = e^{i\pi(2m-1)/N}, \quad \sigma_k^{(\text{as})} = \mathcal{O}(\epsilon^{-1/(N-2)}), \quad (5.10)$$

where  $m = 1, \dots, N$  and  $k = N + 1, \dots, 2(N - 2)$ .

It becomes straightforward to evaluate the hyperelliptic integral in (5.5) for the first set of the branching points in (5.10) (see Appendix B for detail). Combining together (B.13), (B.14) and (5.5) we find the system of  $(N - 2)$  equations for the integrals of motion

$$u_N \cdot N B\left(\frac{1}{2}, \frac{1}{N}\right) - (u_2 u_N)^* \cdot B\left(\frac{1}{2}, \frac{N-1}{N}\right) = \pi \sum_{k=1}^N e^{-i\pi(2k-1)/N} n_k,$$

$$(u_{N+1-m} u_N) \cdot B\left(\frac{1}{2}, \frac{m}{N}\right) - (u_{m+1} u_N)^* \cdot B\left(\frac{1}{2}, \frac{N-m}{N}\right) = \pi \sum_{k=1}^N e^{-i\pi(2k-1)m/N} n_k, \quad (5.11)$$

with  $m = 2, \dots, N - 2$ . Here  $B(x, y) = \Gamma(x)\Gamma(y)/\Gamma(x+y)$  is the Euler beta-function, the moduli  $u_m$  were defined in (5.9) for  $2 \leq m \leq N - 1$  and  $u_N = (q_N/4)^{1/N}$ . One also gets the following relation for the quasimomentum

$$\ell = - \sum_{m=1}^N n_m \pmod{N}. \quad (5.12)$$

These relations were obtained in the small- $\epsilon$  limit and they hold up to corrections  $\sim \epsilon^{3/2}$ . Notice that the sums in r.h.s. of Eqs. (5.11) and (5.12) depend only on a subset of integers  $n_1, \dots, n_{2N-4}$  corresponding to the first set of the branching points in (5.10). Comparing the same small- $\epsilon$  asymptotics of the both sides of (5.11) one finds that  $n_k \sim \epsilon^{-1/2}$ . Then, Eq. (5.6) leads to  $\ell_k \sim \epsilon^{-1/2}$ .

Replacing in (5.11) the moduli  $u_n$  by their explicit expressions (5.9), one obtains the system of  $(N - 2)$  equations for the integrals of motion  $q_3, \dots, q_N$ . Since the second relation in (5.11) is invariant under  $m \rightarrow N - m$ , the number of independent relations reduces to  $(N - 1)$  real equations and, therefore, the system (5.11) is undetermined. The remaining quantization conditions follow from the analysis of the integral (5.5) for the second set of the branching points in Eq. (5.10). A straightforward calculation shows that the corresponding  $n$ -integers, entering the r.h.s. of (5.5), scale in the limit (5.7) as  $n_k \sim \epsilon^{1/2}$  and induce subleading WKB corrections.

The quantized values of the ‘‘highest’’ charge  $q_N$  can be calculated from the first relation in (5.11). One finds after some algebra the following remarkable expression

$$q_N^{1/N} = \pi \frac{\Gamma(1 + 2/N)}{\Gamma^2(1/N)} \mathcal{Q}(\mathbf{n}) \left[ 1 + \frac{q_2^*}{\pi} \frac{2N^2}{N-2} \cot(\pi/N) |\mathcal{Q}(\mathbf{n})|^{-2} + \mathcal{O}(|\mathcal{Q}(\mathbf{n})|^{-4}) \right], \quad (5.13)$$

where the notation was introduced for the Fourier series

$$\mathcal{Q}(\mathbf{n}) = \sum_{k=1}^N n_k e^{-i\pi(2k-1)/N}, \quad (5.14)$$

and  $q_2^* = 1/4 + (\nu_h + in_h/2)^2 - N(\nu_s + in_s/2)^2$  according to (1.5).

The sum in the r.h.s. of (5.14) is invariant under simultaneous shift of integers,  $n_k \rightarrow n_k + a$ . This transformation changes the value of  $\ell$  in Eq. (5.12), but leaves invariant the quasimomentum  $\theta_N = \exp(2\pi i \ell / N)$ . Therefore,  $q_N^{1/N}$  and  $\theta_N$  depend on the differences  $n_k - n_{k+1}$ , which in their

turn can be expressed in terms of the  $\ell$ -integers with a help of (5.6). To obtain the corresponding expressions for  $q_N^{1/N}$  and  $\theta_N$  one chooses the “gauge”  $n_1 = 0$  and substitutes in (5.14) and (5.12)

$$n_{2k} = -\ell_{2k}, \quad n_{2k+1} = \ell_{2k-1} - \ell_{2k}, \quad (5.15)$$

with  $k = 1, \dots, N-2$ . It follows from (5.13) that, to the leading order of the WKB expansion,  $q_N^{1/N}$  does not depend on the total  $SL(2, \mathbb{C})$  spin  $h = (1 + n_h)/2 + i\nu_h$ . The  $h$ -dependence enters into (5.13) through the nonleading correction, which becomes smaller as one goes to higher excited states with larger  $n_k$ .

### 5.1.1. Special case: $N = 3$

For  $N = 3$  we find from (5.13) and (5.12) the quantized values of the charge  $q_3$

$$q_3^{1/3} = \frac{\Gamma^3(2/3)}{2\pi} \left[ \frac{1}{2}(n_1 - 2n_2 + n_3) + i\frac{\sqrt{3}}{2}(n_3 - n_1) \right] + \mathcal{O}(\epsilon^{1/2}), \quad (5.16)$$

and the quasimomentum  $\ell = -n_1 - n_2 - n_3$ , with  $n_{1,2,3} \sim \epsilon^{-1/2}$ . Here, for simplicity we did not include the nonleading correction  $\sim q_2^*$ . Using (5.6) one rewrites these relations as<sup>3</sup>

$$\begin{aligned} q_3^{1/3}(\ell_1, \ell_2) &= \frac{\Gamma^3(2/3)}{2\pi} \left[ \frac{1}{2}(\ell_1 + \ell_2) + i\frac{\sqrt{3}}{2}(\ell_1 - \ell_2) \right], \\ \theta_3(\ell_1, \ell_2) &= -\frac{2\pi}{3}(\ell_1 + \ell_2) \pmod{2\pi}. \end{aligned} \quad (5.17)$$

Thus, to the leading order of the WKB expansion, the quantized charges  $q_3^{1/3}(\ell_1, \ell_2)$  are located on the complex plane at the vertices of the lattice built from equilateral triangles.

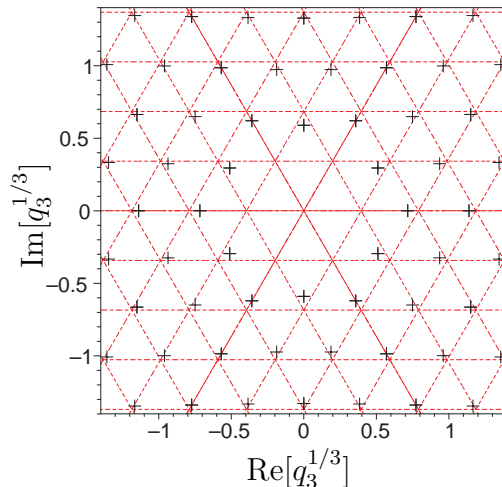


Figure 4: Lattice structure at  $N = 3$ . Crosses denote the exact values of  $q_3^{1/3}$  at  $q_2 = 1/4$ . Dotted lines intersect at the points defined in Eq. (5.17).

As one can see from Figure 4, Eq. (5.17) is in a good agreement with the exact results. Notice however that the exact values of  $q_3$  do not approach the origin, so that a few lattice vertices

<sup>3</sup>To make the correspondence with Ref. [10], one has to redefine integers as  $\ell_1 + \ell_2 \rightarrow \ell_1$  and  $\ell_1 - \ell_2 \rightarrow \ell_2$ .



remain vacant. Since the corresponding  $q_3$  are small, one should not expect the WKB approach to be applicable in this region. Indeed, one can verify that for  $|q_3| < \Delta_3$ , the first nonleading WKB correction to the periods  $a(q_3)$  and  $a_D(q_3)$  becomes comparable with the leading order contribution.

### 5.1.2. Special case: $N = 4$

For  $N = 4$  the spectrum of the magnet is parameterized by two quantum numbers  $q_3$  and  $q_4$ . From (5.13) one gets the charge  $q_4$  as

$$q_4^{1/4} = \frac{\Gamma^2(3/4)}{4\sqrt{\pi}} \left[ \frac{1}{\sqrt{2}}(n_1 - n_2 - n_3 + n_4) + \frac{i}{\sqrt{2}}(-n_1 - n_2 + n_3 + n_4) \right] + \mathcal{O}(\epsilon^{1/2}), \quad (5.18)$$

where, in general,  $n_{1,2,3,4} = \mathcal{O}(\epsilon^{-1/2})$ . The quasimomentum (5.12) is equal to

$$\theta_4 = -\frac{\pi}{2}\ell = \frac{\pi}{2}(n_1 + n_2 + n_3 + n_4) \pmod{2\pi}. \quad (5.19)$$

To find the charge  $q_3$ , we apply the second relation in (5.11) at  $N = 4$ ,  $m = 2$  and use the definition of the moduli (5.9)

$$\text{Im} \frac{q_3}{q_4^{1/2}} = (-n_1 + n_2 - n_3 + n_4) + \mathcal{O}(\epsilon^{3/2}). \quad (5.20)$$

As was already explained, the system (5.11) is undetermined and it does not fix the charge  $q_3$  completely. The additional relation on  $q_3$  comes from the analysis of the branching points in (5.10) located far from the origin.

The solutions to (5.18) and (5.20) are parameterized by three integers  $\ell_1 = n_3 - n_2$ ,  $\ell_2 = n_1 - n_2$  and  $\ell_4 = n_1 - n_4$ . To reveal the properties of the spectrum it is more convenient, however, to introduce their linear combinations

$$\begin{aligned} m_1 &= (n_1 - n_2 - n_3 + n_4)/2 = (n_1 + n_4) + \frac{\ell}{2}, \\ m_2 &= (-n_1 - n_2 + n_3 + n_4)/2 = (n_3 + n_4) + \frac{\ell}{2}, \end{aligned} \quad (5.21)$$

where integer  $\ell$  defines the quasimomentum (5.19). Notice that  $m_{1,2}$  are integer for  $\ell = \text{even}$  and half-integer for  $\ell = \text{odd}$ . Choosing the gauge  $n_1 = 0$ , one rewrites (5.18) and (5.20) as

$$\begin{aligned} q_4^{1/4} &= \frac{\Gamma^2(3/4)}{2\sqrt{\pi}} \left( \frac{m_1}{\sqrt{2}} + i \frac{m_2}{\sqrt{2}} \right) + \mathcal{O}(\epsilon^{1/2}), \\ \text{Im} \frac{q_3}{q_4^{1/2}} &= 2 \left( m_1 - m_2 - \frac{\ell}{2} \right) + \mathcal{O}(\epsilon^{3/2}), \end{aligned} \quad (5.22)$$

where  $m_1 = (-\ell_1 + 2\ell_2 - \ell_4)/2$ ,  $m_2 = (\ell_1 - \ell_4)/2$  and  $m_{1,2} = \mathcal{O}(\epsilon^{-1/2})$ . Let us examine these expressions in more detail. It is convenient to consider separately the  $N = 4$  eigenstates with  $q_3 = 0$  and  $q_3 \neq 0$ .

For the eigenstates with  $q_3 = 0$  one finds from (5.20) that  $n_1 + n_3 = n_2 + n_4$ . As a consequence, their quasimomentum,  $\theta_4 = -\pi\ell/2 = \pi(n_1 + n_3)$ , takes the values  $\theta_4 = 0, \pi \pmod{2\pi}$ , while

$m_1 = n_1 - n_2$  and  $m_2 = n_3 - n_2$  are strictly integer. Thus, the quantized values of  $q_4$  for the eigenstates with  $q_3 = 0$  are described by the first relation in (5.22) with  $m_{1,2}$  integer. They form a square lattice on the complex  $q_4^{1/4}$ -plane whose vertices are specified by the pair of integers  $(m_1, m_2)$ . For  $m_1 \pm m_2 = \text{even}$ ,  $\ell = 0 \pmod{4}$  and the quasimomentum equals  $\theta_4 = 0$ . For  $m_1 \pm m_2 = \text{odd}$ ,  $\ell = 2 \pmod{4}$  and the quasimomentum equals  $\theta_4 = \pi$ .

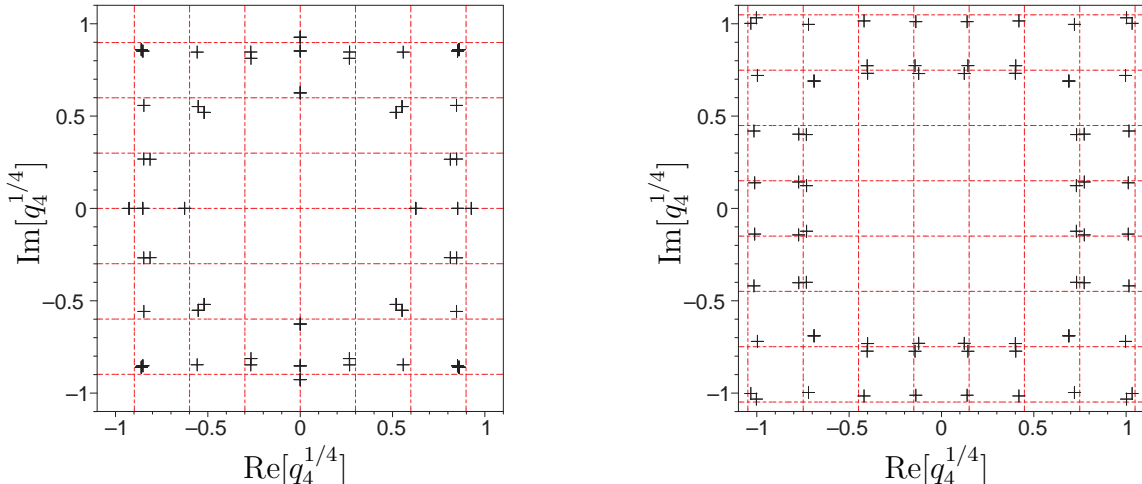


Figure 5: Lattice structure at  $N = 4$ . Crosses denote the exact values of  $q_4^{1/4}$  for different  $q_3$  and  $q_2 = 1/4$ . Dotted lines intersect at the points defined in Eq. (5.22) with  $m_{1,2}$  integer (left panel) and  $m_{1,2}$  half-integer (right panel).

For  $q_3 \neq 0$  the eigenstates can be separated into two groups according to their quasimomentum,  $\theta_4 = 0, \pi$  and  $\theta_4 = \pm\pi/2$ . Let us visualize the solutions to (5.22) as points on the three-dimensional  $\xi$ -space with the coordinates  $\xi_1 = \text{Re} q_4^{1/4}$ ,  $\xi_2 = \text{Im} q_4^{1/4}$  and  $\xi_3 = \text{Im} (q_3/q_4^{1/2})$ .

- $\theta_4 = 0, \pi$ : One finds from (5.21) and (5.19) that  $\ell$  is even and  $m_{1,2}$  are *integer*. According to (5.22),  $q_4^{1/4}$  does not depend on  $\ell$ . Therefore, choosing  $2(m_1 - m_2) - \ell = 0, \pm 2, \pm 4, \dots$ , one finds that the solutions to (5.22) define an infinite set of identical square lattices in the  $\xi$ -space. These lattices run parallel to the  $(\xi_1, \xi_2)$ -plane, as shown in Figure 5 on the left, and cross the  $\xi_3$ -axis at  $\xi_3 = 0, \pm 2, \pm 4, \dots$ . Exact results indicate that the degeneracy between lattices with different  $\xi_3$  is lifted by nonleading WKB corrections to  $q_3$  and  $q_4$ .
- $\theta_4 = \pm\pi/2$ : One finds from (5.21) and (5.19) that  $\ell$  is odd and  $m_{1,2}$  are *half-integer*. The solutions to (5.22) define an analogous lattice structure in the  $\xi$ -space. The charges  $q_4^{1/4}$  form square lattices on the  $(\xi_1, \xi_2)$ -plane, shown in Figure 5 on the right, which are dual to the similar lattice in the previous case and have the coordinates  $\xi_3 = \pm 1, \pm 3, \pm 5, \dots$

As follows from Figure 5, Eq. (5.22) is in a good agreement with the exact results of Refs. [9, 10].<sup>4</sup> Surprisingly enough, Eq. (5.22) works throughout the whole spectrum including the ground state. The latter is located at  $q_3 = 0$  and  $q_4$  given by (5.22) for  $m_1 = 2$  and  $m_2 = 0$ . Similar to the  $N = 3$  case, a few lattice sites remain unoccupied in the small  $q_4$  region, where the WKB approach is not applicable.

<sup>4</sup>At the same time, Eq. (5.22) invalidates the claim of Refs. [24, 26] that the charge  $q_4$  may take only real values.

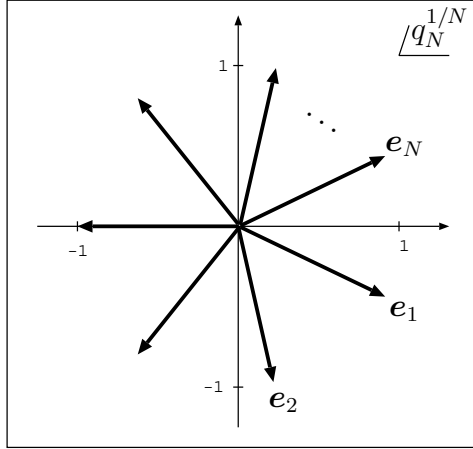


Figure 6: Lattice structure on the complex  $q_N^{1/N}$ -plane is defined by linear integer combinations of the vectors  $\mathbf{e}_1, \dots, \mathbf{e}_N$ .

Going over to higher  $N$ , we find that the lattice structure becomes more complicated. The leading order expression for the “highest” charge, Eq. (5.13), can be written in the vector form

$$q_N^{1/N} = \pi \frac{\Gamma(1 + 2/N)}{\Gamma^2(1/N)} \cdot \sum_{k=1}^N n_k \mathbf{e}_k + \mathcal{O}(\epsilon^{1/2}), \quad (5.23)$$

where  $\mathbf{e}_k \equiv e^{-i\pi(2k-1)/N}$  define unit vectors on the complex plane as shown in Figure 6. The quantized values of  $q_N^{1/N}$  are given by linear combinations of these vectors with integer (positive and negative) weights. Since  $\sum_{k=1}^N \mathbf{e}_k = 0$ , the charge  $q_N^{1/N}$  depends on the differences  $n_k - n_{k+1}$ , or equivalently on the  $\ell$ -integers, Eq. (5.6).

## 5.2. Whitham flow

In the previous Section, we solved the quantization conditions (3.23) in the limit (5.7), which corresponds to large charges  $q_3, \dots, q_N$  and fixed  $q_2$ , or equivalently the total  $SL(2, \mathbb{C})$  spin  $h = (1 + n_h)/2 + i\nu_h$ . Let us now determine the dependence of the charges (1.4) on the continuous parameter  $\nu_h$ .

To simplify analysis, we choose a single particle spin in (1.5) as  $s = 0$  and consider the limit  $\nu_h \gg n_h$ . One finds from (1.5) that  $q_2 = 1/4 + \nu_h^2$  takes large positive values in this limit.<sup>5</sup> Let us explore an ambiguity in choosing the WKB parameter  $\eta$  in Eqs. (3.1) and (3.23) and fix it as

$$\eta = q_2^{-1/2} = (1/4 + \nu_h^2)^{-1/2}, \quad \hat{q}_n = q_n q_2^{-n/2}, \quad (5.24)$$

with  $n = 2, \dots, N$ , so that  $\hat{q}_2 = 1$ . In this Section, we shall solve the quantization conditions (3.23) and determine the dependence of quantized  $\hat{q}_n$  on  $\eta$ . As an example, we present in Figure 7 the dependence  $\hat{q}_3 = \hat{q}_3(\nu_h; \ell_1, \ell_2)$  at  $N = 3$  for different trajectories. We will show below that the  $\nu_h$ -dependence of the charges is governed by the Whitham equations [27].

<sup>5</sup>One can also consider the limit  $n_h \gg \nu_h$ , so that  $q_2 = 1/4 - n_h^2/4$  is negative. Similar analysis allows one to find the  $n_h$ -dependence of the quantum numbers  $q_n$ .

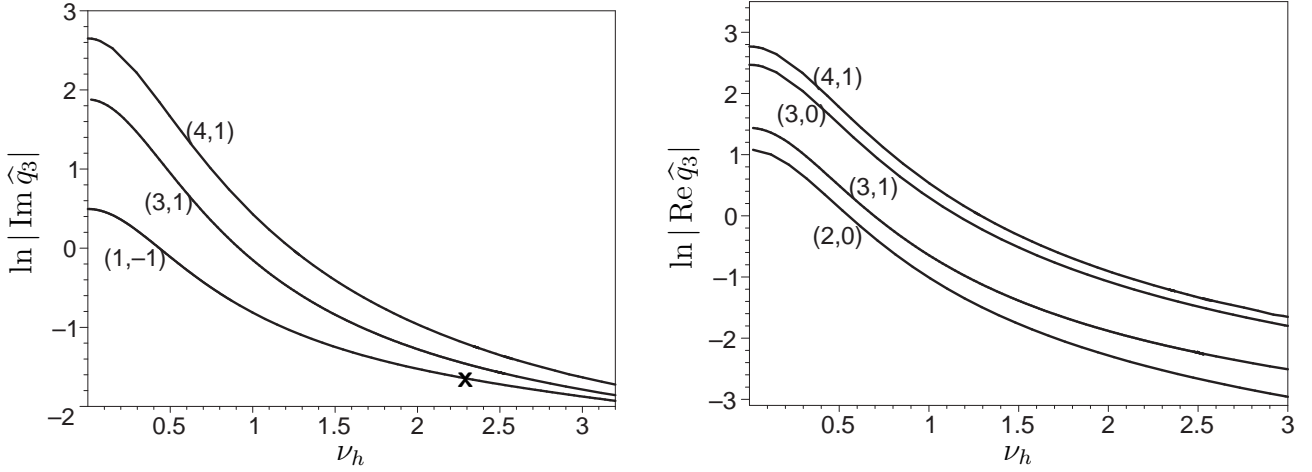


Figure 7: The dependence of  $\hat{q}_3 = q_3/q_2^{3/2}$  on the total spin  $h = 1/2 + i\nu_h$  along different trajectories specified by integers  $(\ell_1, \ell_2)$ . The charge  $\hat{q}_3$  takes real values along the  $(2, 0)$ – and  $(3, 0)$ –trajectories, and pure imaginary values along the  $(1, -1)$ –trajectory. Cross denotes a point with  $\hat{q}_3 = \pm i/\sqrt{27}$ .

### 5.2.1. Whitham equations

Derivation of the Whitham equations is based on the following property of the “action”  $S_0(x)$ , Eq. (3.6), [28]

$$\frac{\partial}{\partial \eta} S_0(x) = \int_{x_0}^x dx \frac{\partial p_x}{\partial \eta} = \int_{x_0}^x \frac{dx}{y(x)} \frac{\partial \hat{t}_N(x)}{\partial \eta} = \sum_{k=3}^N \frac{\partial \hat{q}_k}{\partial \eta} \int_{x_0}^x \frac{dx x^{N-k}}{y(x)}, \quad (5.25)$$

where  $\hat{t}_N(x) = 2x^N + x^{N-2} + \sum_{k=3}^N \hat{q}_k x^{N-k}$  and  $y(x)$  was defined in (3.5). Differentiating the both sides of the first relation in (3.23) and taking into account (5.25), one finds after some algebra

$$\operatorname{Re} \left[ \sum_{j=3}^N \partial_\eta \hat{q}_j \cdot \oint_{\alpha_k} \frac{dx x^{N-j}}{y(x)} \right] = \pi \ell_{2k-1}. \quad (5.26)$$

The second equation in (3.23) leads to a similar relation with  $\alpha_k \rightarrow \beta_k$  and  $\ell_{2k-1} \rightarrow \ell_{2k}$ . The l.h.s. of (5.26) involves a (unnormalized) differential of the first kind on  $\Gamma_N$ . Its  $\alpha$ – and  $\beta$ –periods can be parameterized as

$$\oint_{\alpha_k} \frac{dx x^{j-1}}{y(x)} = 2\pi [U^{-1}(\hat{q})]_{jk}, \quad \oint_{\beta_k} \frac{dx x^{j-1}}{y(x)} = 2\pi [U^{-1}(\hat{q}) \cdot \tau(\hat{q})]_{jk}, \quad (5.27)$$

where  $j, k = 1, \dots, N-2$ . Here  $\tau = [\tau_{jk}(\hat{q})]$  is the Riemann matrix for the hyperelliptic curve  $\Gamma_N$ , while the matrix  $U = [U_{kj}(\hat{q})]$  defines the normalized holomorphic differentials (see Eq. (C.1) in Appendix B). Both matrices depend on the charges  $\hat{q}_n$  and are independent from the flow parameter  $\eta$ . In addition, the Riemann  $\tau$ –matrix is symmetric and has positively definite imaginary part [22].

To solve (5.26) one considers linear combinations  $X_k = \sum_{j=1}^{N-2} \partial_\eta \hat{q}_{N+1-j} [U^{-1}(\hat{q})]_{jk}$ . They satisfy the relations

$$2 \operatorname{Re} X_k = \ell_{2k-1}, \quad 2 \operatorname{Re} \sum_{j=1}^{N-2} X_j \tau_{jk} = \ell_{2k}, \quad (5.28)$$

whose solution can be written in the matrix form as

$$\mathbf{X}(\widehat{q}) = -\frac{i}{2\operatorname{Im}\tau} (\boldsymbol{\ell}_{\text{even}} - \tau^\dagger \cdot \boldsymbol{\ell}_{\text{odd}}) = -(\boldsymbol{\ell}_{\text{even}}^t - \boldsymbol{\ell}_{\text{odd}}^t \cdot \tau^\dagger) \frac{i}{2\operatorname{Im}\tau}, \quad (5.29)$$

where the vectors  $\boldsymbol{\ell}_{\text{even}}$  ( $\boldsymbol{\ell}_{\text{odd}}$ ) are built from integers  $l_{2k}$  ( $l_{2k-1}$ ), and  $\operatorname{Im}\tau = (\tau - \tau^\dagger)/(2i)$  is a positively definite symmetric matrix. Finally, one replaces  $\mathbf{X}(\widehat{q})$  in (5.29) by its definition, puts  $\eta = q_2^{-1/2}$  and finds the system of Whitham equations

$$q_2^{3/2} \frac{\partial \widehat{q}_n}{\partial q_2} = \frac{i}{4} \left[ (\boldsymbol{\ell}_{\text{even}}^t - \boldsymbol{\ell}_{\text{odd}}^t \cdot \tau^\dagger(\widehat{q})) \frac{1}{\operatorname{Im}\tau(\widehat{q})} \cdot U(\widehat{q}) \right]_{N+1-n} \quad (5.30)$$

with  $n = 3, \dots, N$ . Notice that the r.h.s. of (5.30) is  $q_2$ -independent and it depends only on the charges  $\widehat{q}_n$ .

The Whitham equations (5.30) involve the matrices  $U(\widehat{q})$  and  $\tau(\widehat{q})$  defined in (5.27). Their explicit expressions depend on the choice of the canonical set of the oriented cycles on  $\Gamma_N$ . As was already mentioned, the  $\alpha$ - and  $\beta$ -periods are defined up to transformation (5.1), which acts on  $U(\widehat{q})$  and  $\tau(\widehat{q})$  as

$$U \rightarrow (a + b\tau)^{-1}U, \quad \tau \rightarrow (c + b\tau)(a + b\tau)^{-1}. \quad (5.31)$$

It is easy to verify that the Whitham equations (5.30) are invariant under (5.31) provided that  $\boldsymbol{\ell}_{\text{odd}}$  and  $\boldsymbol{\ell}_{\text{even}}$  are transformed according to (5.3).

The Whitham equations (5.30) describe the dependence of the charges,  $q_n = q_n(\nu_h, \boldsymbol{\ell})$  on the total spin of the system  $\nu_h$ . They define the flow of the quantum numbers  $q_n$  with  $\nu_h$  along the trajectory labelled by the integers  $\boldsymbol{\ell}$  (see Figure 3). To solve (5.30) one has to specify the initial conditions for  $\widehat{q}_n$  (with  $n = 3, \dots, N$ ) at some reference  $q_2$ . They are provided by the expressions for the charges  $q_n$ , Eqs. (5.13) and (5.23), obtained in the previous section. We recall that Eqs. (5.13) and (5.23) were obtained in the region of the moduli space (5.7) corresponding to  $q_2 = \text{fixed}$ . The Whitham equations (5.30) allow us to evolve the charges  $q_n$  to arbitrary large values of  $q_2$ .

### 5.2.2. Whitham flow at $N = 3$

In the rest of this section, we shall present a detailed analysis of the Whitham equations at  $N = 3$ . Generalization to higher  $N$  is straightforward and can be performed along the same lines.

At  $N = 3$  it is convenient to introduce notation for the periods of the action differential (3.6)

$$a(\widehat{q}_3) = \frac{1}{2\pi} \oint_{\alpha} dx \frac{(2x + 3\widehat{q}_3)}{y(x)}, \quad a_D(\widehat{q}_3) = \frac{1}{2\pi} \oint_{\beta} dx \frac{(2x + 3\widehat{q}_3)}{y(x)}. \quad (5.32)$$

Here integration goes over the  $\alpha$ - and  $\beta$ -cycles on the elliptic curve  $\Gamma_3$ , Eq. (1.10)

$$\Gamma_3 : \quad y^2(x) = (x + \widehat{q}_3)(4x^3 + x + \widehat{q}_3) = 4 \prod_{j=1}^4 (x - \sigma_j). \quad (5.33)$$

The genus of the Riemann surface defined by  $\Gamma_3$  equals  $g = N - 2 = 1$ . The quantization conditions (3.23) for the charge  $\widehat{q}_3 = q_3/q_2^{3/2}$  look like

$$\operatorname{Re} a(\widehat{q}_3) = \frac{\ell_1}{2q_2^{1/2}}, \quad \operatorname{Re} a_D(\widehat{q}_3) = \frac{\ell_2}{2q_2^{1/2}}. \quad (5.34)$$

The Whitham equations (5.30) take the following form at  $N = 3$

$$q_2^{3/2} \frac{\partial \widehat{q}_3}{\partial q_2} = i \frac{\ell_2 - \ell_1 \tau^*(\widehat{q}_3)}{4 \operatorname{Im} \tau(\widehat{q}_3)} U(\widehat{q}_3), \quad (5.35)$$

with the functions  $U(\widehat{q}_3)$  and  $\tau(\widehat{q}_3)$  defined from (5.27) and (5.25) as

$$U(\widehat{q}_3) = \frac{1}{a'(\widehat{q}_3)} = 2\pi \left( \oint_{\alpha} \frac{dx}{y(x)} \right)^{-1}, \quad \tau(\widehat{q}_3) = \frac{a'_D(\widehat{q}_3)}{a'(\widehat{q}_3)} = \frac{\oint_{\beta} dx/y(x)}{\oint_{\alpha} dx/y(x)}, \quad (5.36)$$

where  $a'(\widehat{q}_3) = \partial a(\widehat{q}_3)/\partial \widehat{q}_3$  and similar for  $a'_D$ . We recall that  $\operatorname{Im} \tau(\widehat{q}_3) > 0$  for arbitrary  $\widehat{q}_3$ .

Performing integration in the r.h.s. of (5.32), one can evaluate  $a(\widehat{q}_3)$  and  $a_D(\widehat{q}_3)$  in terms of the elliptic function of the first and the second kinds. The resulting expressions for  $a(\widehat{q}_3)$  and  $a_D(\widehat{q}_3)$  are analytical functions on the complex  $\widehat{q}_3$ -plane with two cuts. The cuts start at the values of  $\widehat{q}_3$ , for which any two branching points of the curve  $\Gamma_3$  merge,  $\sigma_j = \sigma_k$ , and the integrand in (5.32) develops a pole. This happens for  $q_3 \rightarrow \infty$ . The remaining singular points correspond to zeros of the discriminant of the polynomial in the r.h.s. of (5.33),

$$16 \prod_{j>k} (\sigma_j - \sigma_k)^2 = -\widehat{q}_3^6 (1 + 27\widehat{q}_3^2). \quad (5.37)$$

In this way, one finds another three singular points on the complex  $\widehat{q}_3$ -plane

$$\widehat{q}_{3,\text{sing}} = -\frac{i}{\sqrt{27}}, \quad 0, \quad \frac{i}{\sqrt{27}}. \quad (5.38)$$

Thus, the two cuts run on the complex  $\widehat{q}_3$ -plane between these three points and  $q_3 = \infty$ . As we will show below, the solutions to the quantization conditions (5.34) can be obtained in a closed form at the vicinity of these points. Let us determine the asymptotic behaviour of the functions  $a(\widehat{q}_3)$  and  $a_D(\widehat{q}_3)$  around the singular points,  $\widehat{q}_3 = 0$ ,  $-i/\sqrt{27}$  and  $\infty$ . The behaviour around  $\widehat{q}_3 = i/\sqrt{27}$  can be found by making use of the symmetry of the curve (5.33) under  $x \rightarrow -x$  and  $\widehat{q}_3 \rightarrow -\widehat{q}_3$ .

As the starting point, one has to specify the  $\alpha$ - and  $\beta$ -cycles on the curve  $\Gamma_3$  (see Figure 1). It is convenient to choose them in such a way that the  $\alpha$ - and  $\beta$ -cycles shrink into a point for  $\widehat{q}_3 \rightarrow -i/\sqrt{27}$  and  $\widehat{q}_3 \rightarrow 0$ , respectively. Obviously, this choice is not unique and one can use another definition of the cycles. The resulting expressions for the periods  $a(\widehat{q}_3)$  and  $a_D(\widehat{q}_3)$  are related to each other by the  $SL(2, \mathbb{Z})$  transformation (5.1) and (5.3).

At  $q_3 = 0$  the branching points are located along the imaginary axis at  $\sigma_1 = \sigma_2 = 0$ ,  $\sigma_3 = i/2$  and  $\sigma_4 = -i/2$ . According to our definition of the cycles, Figure 1, the  $\alpha$ -cycle encircles the cut  $[\sigma_2, \sigma_3]$ , whereas the  $\beta$ -cycle shrinks into a point. Calculation of (5.32) leads to

$$a_D(0) = 0, \quad a(0) = \frac{1}{\pi} \oint_{\alpha} \frac{dx}{\sqrt{4x^2 + 1}} = \frac{2}{\pi} \int_0^{i/2} \frac{dx}{\sqrt{4x^2 + 1}} = \frac{i}{2}. \quad (5.39)$$

To obtain the behaviour of the functions  $a(\widehat{q}_3)$  and  $a_D(\widehat{q}_3)$  in the vicinity of  $\widehat{q}_3 = 0$ , one examines their derivatives with respect to  $\widehat{q}_3$ . According to (5.25), they are given by the  $\alpha$ - and  $\beta$ -periods of the holomorphic differential  $dx/y(x)$  on  $\Gamma_3$ , which can be calculated by the standard methods.

The details of the calculations can be found in [17]. In this way, one obtains the asymptotic behaviour of the periods around  $\widehat{q}_3 = 0$  as

$$\begin{aligned} a(\widehat{q}_3) &= \frac{i}{2} - \frac{3}{\pi} \widehat{q}_3 [\ln(i\widehat{q}_3) - 1] + \dots, \\ a_D(\widehat{q}_3) &= i\widehat{q}_3 + \dots, \end{aligned} \quad (5.40)$$

where ellipses denote subleading  $\mathcal{O}(\widehat{q}_3^2)$ -terms.

At  $\widehat{q}_3 = -i/\sqrt{27}$  the branching points are located at  $\sigma_3 = \sigma_2 = i/\sqrt{12}$ ,  $\sigma_1 = i/\sqrt{27}$  and  $\sigma_4 = -i/\sqrt{3}$ . The  $\beta$ -cycle encircles  $\sigma_2$  and  $\sigma_1$ , while the  $\alpha$ -cycle shrinks into a point (see Figure 1). The periods (5.32) are given by

$$a(-i/\sqrt{27}) = 0, \quad a_D(-i/\sqrt{27}) = \frac{1}{\pi} \int_{i/\sqrt{27}}^{i/\sqrt{12}} \frac{dx}{\sqrt{(x+i/\sqrt{3})(x-i/\sqrt{27})}} = \frac{\ln 2}{\pi}. \quad (5.41)$$

Expanding the periods in the vicinity of  $\widehat{q}_3 = -i/\sqrt{27}$  one finds

$$\begin{aligned} a(\widehat{q}_3) &= \frac{i}{3}(1 - \widehat{q}_3/q) + \dots, \\ a_D(\widehat{q}_3) &= \frac{\ln 2}{\pi} + \frac{1}{6\pi}(1 - \widehat{q}_3/q) [\ln(1 - \widehat{q}_3/q) - c] + \dots, \end{aligned} \quad (5.42)$$

where  $q = -i/\sqrt{27}$ ,  $c = 1 + \ln(27/2)$  and ellipses denote  $\mathcal{O}((1 - \widehat{q}_3/q)^2)$ -terms.

For  $\widehat{q}_3 \rightarrow \infty$  the branching points  $\sigma_k$  move away from the origin and the spectral curve (5.33) can be approximated as  $y^2 = (x + \widehat{q}_3)(4x^3 + \widehat{q}_3)$ . Three branching points are located at the vertices of equilateral triangle,  $\sigma_k = (\widehat{q}_3/4)^{1/3} e^{i\pi(2k-1)/3}$  with  $k = 1, 2, 3$ , and the last point at  $\sigma_4 = -\widehat{q}_3$ . The calculation of the periods (5.32) leads to

$$\begin{aligned} a(\widehat{q}_3) &\stackrel{\widehat{q}_3 \rightarrow \infty}{=} \widehat{q}_3^{1/3} \frac{2\pi}{3\Gamma^3(2/3)} \cdot \left( \frac{3}{2} - i \frac{\sqrt{3}}{2} \right) + \dots, \\ a_D(\widehat{q}_3) &\stackrel{\widehat{q}_3 \rightarrow \infty}{=} \widehat{q}_3^{1/3} \frac{2\pi}{3\Gamma^3(2/3)} \cdot \left( \frac{3}{2} + i \frac{\sqrt{3}}{2} \right) + \dots, \end{aligned} \quad (5.43)$$

where ellipses denote subleading  $\mathcal{O}(q_3^{-1/3})$ -terms. Notice that (5.43) can be written as  $a(\widehat{q}_3) = (I_3 - I_2)/(2\pi)$  and  $a_D(\widehat{q}_3) = (I_1 - I_2)/(2\pi)$ , where the integral  $I_k$  was defined in (B.12) for  $N = 3$ . We already encountered the same elliptic integral in Section 5.1, when we analyzed the quantization condition in another region of the  $\mathbf{q}$ -space, Eq. (5.7). Matching (5.24) into (5.7) we find that

$$\widehat{q}_3 = \mathcal{O}(\epsilon^{-3/2}), \quad q_2 = \mathcal{O}(\epsilon^0). \quad (5.44)$$

Thus, the two regions, Eqs. (5.7) and (5.24), overlap as  $\widehat{q}_3 \rightarrow \infty$  and  $q_2$  is fixed. As a consequence, one expects that at large  $\widehat{q}_3$  the solutions to the quantization conditions (5.34) should match the expressions for the quantum numbers  $q_3$  obtained in the previous Section, Eq. (5.23). Indeed, substitution of (5.43) into (5.34) yields the expression

$$\widehat{q}_3^{1/3} = q_2^{-1/2} \frac{\Gamma^3(2/3)}{2\pi} \left[ \frac{1}{2}(\ell_1 + \ell_2) + i \frac{\sqrt{3}}{2}(\ell_1 - \ell_2) \right] + \mathcal{O}(q_2^{1/2}), \quad (5.45)$$

which coincides with (5.17) since  $\widehat{q}_3^{1/3} = q_3^{1/3} q_2^{-1/2}$ .

Let us substitute the obtained expressions for the  $a$ - and  $a_D$ -periods into the quantization conditions (5.34) and derive the WKB expression for the charge  $q_3$ . We remind that Eqs. (5.40) and (5.42) hold in the vicinity of  $\widehat{q}_3 = 0$  and  $\widehat{q}_3 = -i/\sqrt{27}$ , respectively.

For  $|\widehat{q}_3| \ll 1$  one finds from (5.40) and (5.34)

$$\text{Im } \widehat{q}_3 = -\frac{1}{2} \ell'_2 q_2^{-1/2}, \quad \text{Re} [\widehat{q}_3 (\ln(i\widehat{q}_3) - 1)] = -\frac{\pi}{6} \ell'_1 q_2^{-1/2}, \quad (5.46)$$

where  $\widehat{q}_3 = q_3/q_2^{3/2}$ . Eq. (5.46) defines the scaling behaviour of quantized  $q_3$  in the region  $q_3 \sim q_2$  for large  $q_2$ . Notice that in comparison with (5.34) we replaced  $(\ell_1, \ell_2)$  by another pair of integers  $(\ell'_1, \ell'_2)$ . This was done in order to distinguish the  $\ell$ -integers entering the r.h.s. of (5.45) and (5.46). As was already mentioned, the periods  $a(\widehat{q}_3)$  and  $a_D(\widehat{q}_3)$  depend on the definition of the  $\alpha$ - and  $\beta$ -cycles on the Riemann surface  $\Gamma_3$ . These cycles encircle the branching points  $\sigma_k$  (see Figure 1), which are moved on the complex plane as  $\widehat{q}_3$  varies. The two pairs of integers,  $(\ell_1, \ell_2)$  and  $(\ell'_1, \ell'_2)$ , would have been the same if, going from  $\widehat{q}_3 \rightarrow \infty$  to  $\widehat{q}_3 = 0$ , we have traced the  $\widehat{q}_3$ -dependence of the  $\alpha$ - and  $\beta$ -cycles. Within our definition of the cycles, the two pairs are related to each other by the  $SL(2, \mathbb{Z})$  transformation (5.3)

$$\ell'_1 = -\ell_1 - \ell_2, \quad \ell'_2 = -\ell_2. \quad (5.47)$$

For  $\widehat{q}_3 \sim q = -i/\sqrt{27}$ , one finds from (5.42) and (5.34)

$$\text{Re } \widehat{q}_3 = \frac{1}{2\sqrt{3}} \ell'_1 q_2^{-1/2}, \quad \text{Re} ((1 - \widehat{q}_3/q) [\ln(1 - \widehat{q}_3/q) - c]) = 3\pi \ell'_2 q_2^{-1/2} - 6 \ln 2, \quad (5.48)$$

with  $(\ell'_1, \ell'_2)$  the same as in (5.46) and (5.47). It follows from this relation that  $\text{Im } \widehat{q}_3 / \text{Re } \widehat{q}_3 \sim \ln q_2$ , so that  $\widehat{q}_3$  is dominated by its imaginary part at large  $q_2$ . Eq. (5.48) defines the scaling behaviour of quantized  $q_3$  in the vicinity of the point on the moduli space  $q_3 = -i(q_2/3)^{3/2}$ .

For  $\widehat{q}_3 \rightarrow \infty$ , the leading order expression for the charge is given by (5.45). One can improve this relation by including nonleading corrections to the periods in (5.42). In this way, we obtain

$$q_3^{1/3} = \frac{\Gamma^3(2/3)}{2\pi} \mathcal{Q}(\mathbf{n}) \left[ 1 + \frac{3\sqrt{3}}{2\pi} \frac{q_2}{|\mathcal{Q}(\mathbf{n})|^2} - \left( \frac{3\sqrt{3}}{2\pi} \frac{q_2}{|\mathcal{Q}(\mathbf{n})|^2} \right)^2 + \mathcal{O}(q_2^3) \right], \quad (5.49)$$

where

$$\mathcal{Q}(\mathbf{n}) = \frac{1}{2}(\ell_1 + \ell_2) + i \frac{\sqrt{3}}{2}(\ell_1 - \ell_2) = \sum_{k=1}^3 n_k e^{i\pi(2k-1)/3}. \quad (5.50)$$

One verifies that the first two terms in the r.h.s. of (5.49) coincide with (5.13) for  $N = 3$  and  $q_2$  real. Eq. (5.49) defines the scaling behaviour of quantized  $q_3$  in the region  $q_3 \gg q_2^{3/2}$ .

By the construction, Eqs. (5.46), (5.48) and (5.49) satisfy the Whitham equation (5.30) in the different regions of the  $(q_2, q_3)$ -space. They define the  $(\ell_1, \ell_2)$ -trajectories, which start at  $q_2 = 1/4$  and go to larger  $q_2 = 1/4 + \nu_h^2$ . Example of such trajectories is shown in Figure 7. In the regions  $q_2 < 1$  and  $q_2 \gg 1$  the charge  $q_3$  satisfies Eqs. (5.49) and (5.46), respectively. Solving the Whitham equation (5.30) and using (5.49) as an initial condition at  $q_2 = 1/4$ , one can reconstruct the flow of  $q_3$  in the intermediate region  $q_2 \sim 1$  along the trajectories labelled



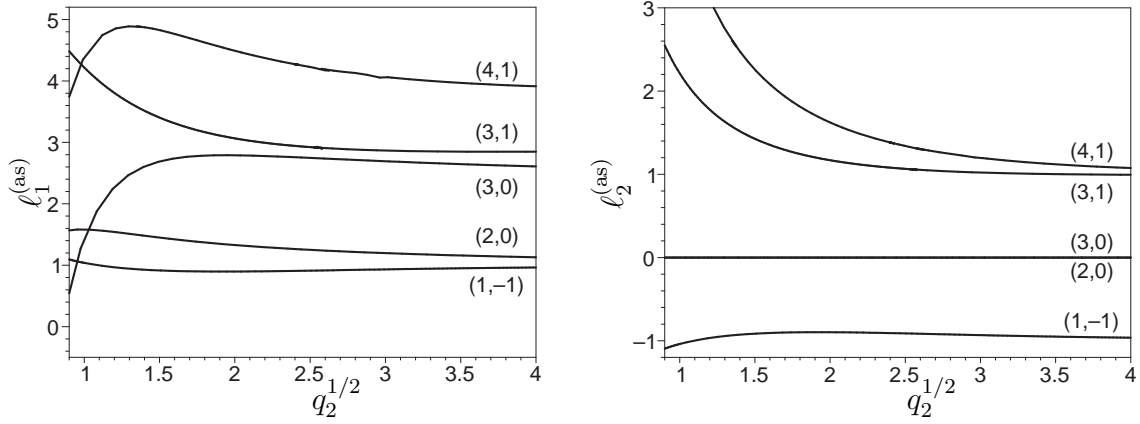


Figure 8: The functions  $\ell_1^{(as)} = \ell'_2 - \ell'_1$  (left panel) and  $\ell_2^{(as)} = -\ell'_2$  (right panel) are calculated from (5.46) using the exact eigenvalues  $q_3$ . Pairs of integers  $(\ell_1, \ell_2)$  attached to the curves specify different trajectories for the charge  $q_3 = q_3(\ell_1, \ell_2)$ , Eq. (5.17).

by integers  $(\ell_1, \ell_2)$ . Some of these trajectories go in the complex  $(q_2, q_3)$ -space in the vicinity of the point  $q_3 = -i(q_2/3)^{3/2}$ . In particular, this is the case for the  $(1, -1)$ -trajectory. The flow of  $q_3$  around this point, shown by cross in Figure 7 (see left panel), is described by Eq. (5.48).

To verify the WKB quantization conditions, one substitutes the exact values of  $q_3$  into the l.h.s. of (5.46) and calculates the corresponding values of  $\ell_{1,2}$  for different  $q_2$  using (5.47). In this way, for each trajectory  $q_3 = q_3(\nu; \ell_1, \ell_2)$  we obtain two functions that we denote as  $\ell_{1,2}^{(as)}(q_2)$ . Few examples of such functions are shown in Figure 8. From (5.46) one would expect that for large  $q_2$  these functions should approach the same integer values  $\ell_{1,2}$  as those specifying the trajectories. Indeed, one finds from Figure 8 that this happens for all trajectories except the  $(2, 0)$ -trajectory. In the latter case, the function  $\ell_1^{(as)}(q_2)$  approaches the value 1 instead of expected  $\ell_1 = 2$ . The reason for this is that the charge  $\hat{q}_3$  takes anomalously small values along the  $(2, 0)$ -trajectory (see Figure 7 on the right). As a consequence, the nonleading WKB correction to the “action” function in (3.2) becomes important for this particular trajectory. It provides a contribution to the  $a(\hat{q}_3)$  and  $a_D(\hat{q}_3)$  comparable with the leading order expression (5.46) and increases the value of  $\ell_1^{(as)}(q_2)$  improving an agreement with the exact result.

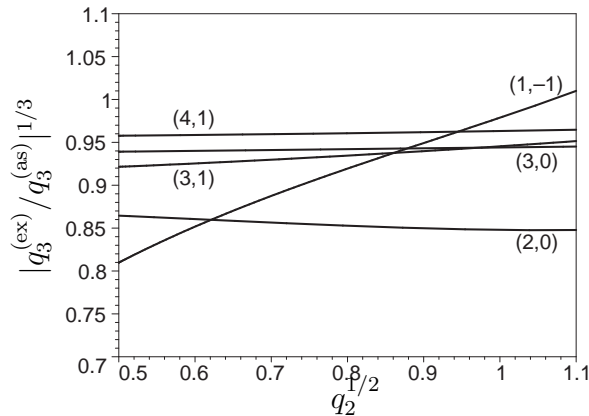


Figure 9: Ratio of the exact,  $q_3^{(ex)}$ , and the asymptotic,  $q_3^{(as)}$ , expressions for the charge  $q_3$  at small  $q_2$ . Different curves correspond to the same trajectories as in Figures 7 and 8.

As can be seen from Figure 8, Eq. (5.46) is not satisfied at small  $q_2$ . To describe the Whitham flow of the charge  $q_3$  in this region, one has to apply (5.49). Comparison of the exact  $q_3$  with the asymptotic expression (5.49) for  $q_2 < 1$  is shown in Figure 9. One observes that, aside from the  $(2, 0)$ -trajectory, the agreement is rather good. The accuracy can be further improved by including nonleading WKB corrections in (3.2).

Thus, the WKB quantization conditions, Eqs. (5.46) and (5.49), successfully describe the exact spectrum of the charge  $q_3$  shown in Figure 7 for  $1/4 \leq q_2 < 1$  and  $q_2 > 1$ , respectively.

## 6. Conclusions

In this paper, we have developed a quasiclassical approach to solving the spectral problem for the noncompact  $SL(2, \mathbb{C})$  Heisenberg spin magnet. It allowed us to understand hidden symmetry properties of the energy spectrum. We also demonstrated that the energy spectrum obtained within this approach is in a good agreement with the exact results.

The model represents a generalization of the well-known spin-1/2 XXX chain to infinite-dimensional representation of the  $SL(2, \mathbb{C})$  group. Using realization of spin operators as differential operators acting on the plane, one can map the noncompact spin magnet of length  $N$  into a two-dimensional completely integrable quantum-mechanical model of  $N$  particles with a nearest-neighbour interaction. This model has appeared in high-energy QCD as describing multi-gluonic compound states in the multi-colour limit. Due to its complete integrability, the energy spectrum of the  $N$  particle system is uniquely specified by the total set of quantum numbers  $q_2, \dots, q_N$ . The latter are defined as eigenvalues of the mutually commuting integrals of motions and their possible values are constrained by the quantization conditions.

Applying the methods of nonlinear WKB analysis [27], we constructed the wave function of the  $N$ -particle system in the representation of the separated coordinates. To the leading order of the WKB expansion, the wave function is determined by the “action” function, which satisfies the Hamiltonian-Jacobi equations in the underlying classical model. In the classical case, the noncompact magnet describes the system of interacting particles moving on the two-dimensional plane. Solving the classical equations of motion, one finds that their collective motion describes a propagation of the soliton wave in the closed chain of particles with periodic boundary conditions. The same motion in the separated coordinates corresponds to wrapping of classical trajectories around the Riemann surface  $\Gamma_N$  defined by spectral curve of the model. The charges  $q_2, \dots, q_N$  take arbitrary complex values in the classical model and define the moduli of  $\Gamma_N$ .

The quantization conditions for the charges  $q_2, \dots, q_N$  follow from the requirement for the wave function of the  $N$ -particle system to be a single-valued function of the separated coordinates. To the leading order of the WKB expansion, these conditions have the form of the Bohr-Sommerfeld relations imposed on periodic orbits of the classical motion on the spectral curve  $\Gamma_N$ . Solving the WKB quantization conditions, we demonstrated that, for fixed total  $SL(2, \mathbb{C})$  spin of the system, the eigenvalues of the integrals of motion form a lattice structure on the moduli space of the model. At  $N = 3$  and  $N = 4$  the lattices are built from equilateral triangles and squares, respectively. The dependence of the charges on the total  $SL(2, \mathbb{C})$  spin is governed by the Whitham equations, which were solved at  $N = 3$  by making use of the modular properties of the elliptic curve  $\Gamma_3$ .

A novel feature of the obtained quantization conditions is that they involve *both* the  $\alpha$ - and  $\beta$ -periods on  $\Gamma_N$ . Notice that in conventional one-dimensional lattice integrable models, like the

$SL(2, \mathbb{R})$  Heisenberg spin magnet and the Toda chain model, the WKB quantization conditions involve only the  $\alpha$ -cycles, since the  $\beta$ -cycles correspond to classically forbidden zones. This implies that the quantization conditions for the  $SL(2, \mathbb{C})$  magnet are invariant under modular transformations of the spectral curve. As a consequence, the energy spectrum of the model possesses a hidden symmetry which is analogous to the  $S$ -duality in the Yang-Mills theory [29].

In conclusion, we should mention that our consideration was restricted to the leading order of the WKB expansion. The obtained expressions for the energy spectrum can systematically improved by including nonleading WKB corrections.

## Acknowledgements

We are most grateful to A. Gorsky and J. Kotański for collaboration at the early stages of this project. We would like to thank R. Janik, I. Kogan, F. Smirnov and A. Turbiner for useful discussions. This work was supported in part by the grant 00-01-005-00 of the Russian Foundation for Fundamental Research (A.M. and S.D.), by the Sofya Kovalevskaya programme of Alexander von Humboldt Foundation (A.M.) and by the NATO Fellowship (A.M.).

## A Appendix: Matching conditions

Let us require that the obtained asymptotic expressions for the Baxter blocks, Eqs. (4.11), (4.13) and (4.15), have to verify the Wronskian condition (4.2). Taking into account (4.15), we obtain after some algebra the following expression for (4.2)<sup>6</sup>

$$\frac{i^N t_N(u)}{\pi} \left[ \sin(\pi(s - iu)) \cdot \varphi_+(u) (\bar{\varphi}_-(u^*))^* - \sin(\pi(s + iu)) \cdot \varphi_-(u) (\bar{\varphi}_+(u^*))^* \right] = 1. \quad (\text{A.1})$$

Together with (4.19) and (4.21), this leads to the following relation for the  $a$ -functions

$$\sin(\pi(s - iu)) \cdot a_+(u) (\bar{a}_-(u^*))^* - \sin(\pi(s + iu)) \cdot a_-(u) (\bar{a}_+(u^*))^* = \text{const}, \quad (\text{A.2})$$

which should hold for arbitrary complex  $u$ .

Another constraint on the  $a$ -functions comes from Eqs. (4.5) and (4.1). It is easy to see that at  $(u = i(1 - s) + \epsilon, \bar{u} = -i\bar{s} + \epsilon)$  and  $(u = -is + \epsilon, \bar{u} = i(1 - \bar{s}) + \epsilon)$  the blocks (4.11), (4.13) and (4.15) have poles in  $\epsilon$  generated by the first term involving  $\varphi_+$ -functions, while the second term proportional to  $\varphi_-$ -functions is suppressed as  $\epsilon^N$ . As a consequence, substituting (4.1) into (4.5) we find that  $\varphi_+(u) \bar{\varphi}_+(\bar{u}) - e^{2i\delta} (\varphi_+(\bar{u}^*) \bar{\varphi}_+(u^*))^*$  has to scale as  $\sim \epsilon^N$  as  $\epsilon \rightarrow 0$  around the above two points. Applying Eqs. (4.19) and (4.21) and taking into account (4.22) we get

$$e^{2i\delta} = \frac{a_+(\pm is + \epsilon) \bar{a}_+(\pm i\bar{s} + \epsilon)}{(a_+(\pm is + \epsilon) \bar{a}_+(\pm i\bar{s} + \epsilon))^*} + \mathcal{O}(\epsilon^N). \quad (\text{A.3})$$

As we will see in a moment (see Eq. (A.11)), this relation is exact and it holds for arbitrary real  $\epsilon$ . This implies in particular that  $\delta$  is real in (4.1).

So far, we have obtained two different asymptotic expressions for the function  $Q(u, \bar{u})$ . One of them follows from the WKB expression for the wave function,  $Q(x/\eta, \bar{x}/\eta)$ , Eq. (3.15). Another

---

<sup>6</sup>In arriving at this relation we neglected terms suppressed by a small parameter (4.10).

one follows from (4.1) after one replaces the  $Q$ -blocks by their expressions, Eqs. (4.11), (4.13) and (4.15). We remind that the two expressions were obtained for large values of the charges  $q_n$ , but in the different regions of parameters,  $x/\eta \gg 1$  and  $u$ -fixed, respectively. Choosing  $u = x/\eta$  and  $\bar{u} = x^*/\eta$ , we notice that Eqs. (3.15) and (4.1) have to coincide for  $x \ll 1$  and  $u \gg 1$ .

To perform the matching, we examine the behaviour of the holomorphic wave functions  $Q_{\pm}(x/\eta)$  in (3.15) for  $u = x/\eta = \text{fixed}$  as  $\eta \rightarrow 0$ . Using Eqs. (3.12), (3.6) and (3.10) and choosing  $x_0 = 0$ , one finds after some algebra

$$Q_{\pm}(u) \sim [t_N(u)u^{(2s-1)N}]^{-1/2} \exp(\pm i\Upsilon(u)), \quad (\text{A.4})$$

where the notation was introduced for the function

$$\Upsilon(u) = u \ln \frac{t_N(u)}{u^N} - \sum_{k=1}^N \lambda_k \ln(\lambda_k - u) + \sum_{k=1}^N \lambda_k \ln \lambda_k, \quad (\text{A.5})$$

with  $\lambda_k$  being the roots of the polynomial  $t_N(u)$  defined in (4.16) and (4.17). Notice that  $\Upsilon(0) = 0$ . To obtain  $\bar{Q}_{\pm}(\bar{x}/\eta)$  one has to replace in (A.4),  $t_N(u) \rightarrow \bar{t}_N(u^*) = (t_N(u))^*$ ,  $s \rightarrow \bar{s} = 1 - s^*$ ,  $\lambda_k \rightarrow \bar{\lambda}_k = \lambda_k^*$ . Then, substituting (A.4) into (3.15) and making use of (3.21), one gets

$$Q(u, u^*) = \text{const} \times |t_N(u)|^{-1} \exp(-iN \text{Arg}(u^{2s-1})) \cos(2 \text{Re} \Upsilon(u) - \Theta), \quad (\text{A.6})$$

where  $\text{Arg}(u^{2s-1}) \equiv -i \ln(u^{2s-1}u^{*2\bar{s}-1})/2$ . This expression should match into (4.1) at large  $u$  and  $\bar{u} = u^*$ .

Let us find the large- $u$  asymptotics of the  $Q$ -blocks, Eqs. (4.11), (4.13) and (4.15). To stay away from the poles of these blocks on the complex  $u$ -plane, we choose  $\text{Re}(1 - s + iu) > 0$ . One gets from (4.20) (up to an inessential overall constant)

$$\begin{aligned} \hat{\varphi}_+(u) \Gamma^N(1 - s + iu) &\sim [t_N(u)u^{(2s-1)N}]^{-1/2} \exp(-i\Upsilon(u) + i\vartheta(u)), \\ \hat{\varphi}_-(u)/\Gamma^N(s + iu) &\sim [t_N(u)u^{(2s-1)N}]^{-1/2} \exp(i\Upsilon(u) - i\vartheta(u)), \end{aligned} \quad (\text{A.7})$$

where  $\Upsilon(u)$  is given by (A.5) and  $\vartheta(u)$  is defined as

$$\vartheta(u) = i\pi u N_- + \sum_{\text{Im} \lambda_k < 0} \lambda_k \ln(i\lambda_k) + \sum_{\text{Im} \lambda_k > 0} \lambda_k \ln(-i\lambda_k), \quad (\text{A.8})$$

with  $N_-$  introduced in (4.23). We observe a striking similarity between (A.7) and (A.4). Identifying the r.h.s. of the first and the second relations in (A.7) as  $Q_{\mp}(u) \exp(\pm i\vartheta(u))$ , respectively, we get from (4.11), (4.13) and (4.15) the following expressions for the holomorphic blocks

$$\begin{aligned} Q_0^{(\text{as})}(u) &\sim a_-(u)Q_+(u) e^{-i\vartheta(u)} + \frac{\sin(\pi(s - iu))}{\pi} a_+(u)Q_-(u) e^{i\vartheta(u)}, \\ Q_1^{(\text{as})}(u) &\sim (\bar{a}_-(u^*))^* Q_+(u) e^{-i\vartheta(u)} + \frac{\sin(\pi(s + iu))}{\pi} (\bar{a}_+(u^*))^* Q_-(u) e^{i\vartheta(u)}, \end{aligned} \quad (\text{A.9})$$

and similar expressions for the antiholomorphic blocks

$$\begin{aligned} \bar{Q}_0^{(\text{as})}(\bar{u}) &\sim \bar{a}_-(\bar{u})\bar{Q}_-(\bar{u}) e^{i\vartheta(\bar{u}^*)^*} + \frac{\sin(\pi(\bar{s} + i\bar{u}))}{\pi} \bar{a}_+(\bar{u})\bar{Q}_+(\bar{u}) e^{-i\vartheta(\bar{u}^*)^*}, \\ \bar{Q}_1^{(\text{as})}(\bar{u}) &\sim (a_-(\bar{u}^*))^* \bar{Q}_-(\bar{u}) e^{i\vartheta(\bar{u}^*)^*} + \frac{\sin(\pi(\bar{s} - i\bar{u}))}{\pi} (a_+(\bar{u}^*))^* \bar{Q}_+(\bar{u}) e^{-i\vartheta(\bar{u}^*)^*}. \end{aligned} \quad (\text{A.10})$$

The functions  $Q_{0,1}^{(\text{as})}(u)$  and  $Q_{\pm}(u)$  approximate the exact solutions to the holomorphic Baxter equation (2.11) in the different regions,  $u \gg 1$  and  $u \sim 1$ , respectively. Eq. (A.9) sews these two sets of functions in the intermediate region of  $u$ .

Let us substitute Eqs. (A.9) and (A.10) into (4.1) and compare the resulting expression for  $Q(u, \bar{u})$  with (3.15) at  $u = x/\eta$  and  $\bar{u} = u^*$ . One finds that  $Q(u, u^*)$  involves four different combinations of the  $Q$ -functions,  $Q_{\pm}\bar{Q}_{\pm}$  and  $Q_{\pm}\bar{Q}_{\mp}$ , whereas the r.h.s. of (3.15) contains only the diagonal terms. To cancel the off-diagonal terms  $\sim Q_{\pm}\bar{Q}_{\mp}$ , one has to require that

$$e^{2i\delta} = \frac{a_+(u)\bar{a}_+(u^*)}{(a_+(u)\bar{a}_+(u^*))^*} = \frac{a_-(u)\bar{a}_-(u^*)}{(a_-(u)\bar{a}_-(u^*))^*}. \quad (\text{A.11})$$

The coefficients  $c_{\pm}$  in front of the diagonal terms  $Q_{\pm}\bar{Q}_{\pm}$  are given by

$$c_+ = \frac{1}{\pi} e^{-2i \operatorname{Re} \vartheta(u) - i\delta} \left[ \sin(\pi(\bar{s} + iu^*)) a_-(u)\bar{a}_+(u^*) - e^{2i\delta} \sin(\pi(\bar{s} - iu^*)) (a_+(u)\bar{a}_-(u^*))^* \right], \quad (\text{A.12})$$

and  $c_- = -c_+^*$ . Eq. (A.12) can be further simplified. Replacing  $\delta$  by its expressions (A.11) and making use of the Wronskian relation (A.2), one gets (up to an overall normalization factor)

$$c_+ = e^{-2i \operatorname{Re} \vartheta(u) - i\delta} \frac{a_-(u)}{(a_-(u))^*} = (-1)^{n_s + n_u} e^{-2i \operatorname{Re} \vartheta(u) - i\delta} \frac{\bar{a}_+(u^*)}{(\bar{a}_+(u^*))^*}. \quad (\text{A.13})$$

Here, in the last relation we applied the identity  $[\sin(\pi(s - iu))]^* = \sin(\pi(1 - \bar{s} + iu^*)) = (-1)^{n_s + n_u} \sin(\pi(s - iu))$  with  $n_u = i(u - u^*)$  integer in virtue of (2.10). Finally, the resulting expression for  $Q(u, u^*)$  matches (A.6) provided that the coefficients  $c_{\pm}$ , Eq (A.12), do not depend on  $u$ . In addition, these coefficients satisfy the relation (3.21),  $c_+/c_- = -c_+/c_+^* = \exp(-2i\Theta)$ , which leads together with (A.13) to

$$c_{\pm} = i e^{\mp i\Theta}, \quad \frac{a_-(u)}{(a_-(u))^*} = (-1)^{n_s + n_u} \frac{\bar{a}_+(u^*)}{(\bar{a}_+(u^*))^*} = i e^{2i \operatorname{Re} \vartheta(u) + i\delta - i\Theta}. \quad (\text{A.14})$$

We recall that these relations hold for  $u$  taking the same values as separated coordinates (2.10), that is  $u = \nu_u - in_u/2$  with  $n_u$  integer and  $\nu_u$  real. For a given set of the integrals of motion, the phases  $\operatorname{Re} \vartheta(u)$  and  $\Theta$  entering (A.14) are uniquely by Eqs. (A.8) and (3.24). In contrast, the phase  $\delta$  depends on the normalization of the blocks. Substituting  $a_{\pm}(u) \rightarrow e^{i\delta/2} a_{\pm}(u)$  and  $\bar{a}_{\pm}(u) \rightarrow e^{i\delta/2} \bar{a}_{\pm}(u)$  in (A.14), one can put  $\delta = 0$  in Eqs. (4.1).

Eqs. (A.14) and (A.11) fix the phases of the  $a$ -functions but not their absolute values. Nevertheless, as shown in Appendix B, this data becomes enough to construct the eigenvalues of the Baxter operator  $Q(u, u^*)$  and to calculate the energy spectrum of the model.

## B Appendix: Calculation of the energy spectrum

In this Appendix we obtain the WKB expressions for the energy and quasimomentum, Eqs. (4.25) and (4.24), respectively.

To begin with, we substitute  $u = \pm is + \epsilon$  and  $\bar{u} = \pm i\bar{s} + \epsilon$  into asymptotic expressions for the  $Q$ -blocks, Eqs. (4.11) and (4.13), and examine the limit  $\epsilon \rightarrow 0$ . One finds that the  $\Gamma$ -functions

in the denominator suppress the contribution of one of the terms in the r.h.s. of (4.11) and (4.13). This leads to the following expression for the quasimomentum (4.7)

$$\theta_N = i \ln \frac{a_+(is)\bar{a}_-(i\bar{s})}{\bar{a}_+(-i\bar{s})a_-(-is)} + i \ln \frac{\widehat{\varphi}_+(is)(\widehat{\varphi}_-(is-i))^*}{\widehat{\varphi}_-(-is)(\widehat{\varphi}_+(i-is))^*} = \theta_N^{(a)} + \theta_N^{(b)}, \quad (\text{B.1})$$

where, for convenience, we split the expression into two pieces. One applies (4.20) and uses the asymptotic behaviour of the  $\Gamma$ -functions at large arguments to get

$$\theta_N^{(b)} = -4 \operatorname{Re} \left[ \sum_{\operatorname{Im} \lambda_k < 0} \lambda_k \ln(i\lambda_k) + \sum_{\operatorname{Im} \lambda_k > 0} \lambda_k \ln(-i\lambda_k) \right]. \quad (\text{B.2})$$

The calculation of  $\theta_N^{(a)}$  goes as follows. One substitutes  $u = \pm is$  into (A.2) and uses anti-periodicity of the function  $\bar{a}_+(u)$ , Eq. (4.22), to obtain  $a_+(is)(\bar{a}_-(i\bar{s}))^* = a_-(-is)(\bar{a}_+(-i\bar{s}))^*$ . This relation allows us to rewrite  $\theta_N^{(a)}$  as

$$\theta_N^{(a)} = i \ln \frac{(a_-(-is))^* a_+(is)}{a_-(-is) (a_+(is))^*} = -2\delta + i \ln \frac{(a_-(-is))^* (\bar{a}_+(i\bar{s}))^*}{a_-(-is) \bar{a}_+(i\bar{s})}, \quad (\text{B.3})$$

where in the second relation we used Eq. (A.11). Then, one takes into account (A.14) and (A.8) to get

$$\theta_N^{(a)} = -2\Theta + 4 \operatorname{Re} \left[ \sum_{\operatorname{Im} \lambda_k < 0} \lambda_k \ln(i\lambda_k) + \sum_{\operatorname{Im} \lambda_k > 0} \lambda_k \ln(-i\lambda_k) \right] \pmod{2\pi}. \quad (\text{B.4})$$

Finally, combining together (B.2) and (B.4) we obtain (4.24).

The calculation of the energy (4.6) goes along the same lines. One substitutes (4.11) and (4.13) into (4.6) and expresses the result in the following form

$$E_N = \left\{ -2 \operatorname{Im} \left( \ln \frac{\widehat{\varphi}_+(is)}{[\widehat{\varphi}_+(i(1-s))]^*} \right)' + \Delta E_N \right\} - 2 \operatorname{Im} \left( \ln \frac{a_+(is)}{\bar{a}_+(-i\bar{s})} \right)' = E_N^{(a)} + E_N^{(b)}. \quad (\text{B.5})$$

Here, the notation was introduced for an additive constant

$$\Delta E_N = -2N \operatorname{Re}[\psi(1-2s) + \psi(1-2\bar{s})] + \varepsilon_N = -4N\psi(1), \quad (\text{B.6})$$

with  $\varepsilon_N$  defined in (4.6) and  $\operatorname{Re} \psi(1-2\bar{s}) = \operatorname{Re} \psi(2s-1)$  in virtue of  $\bar{s} = 1-s^*$ . To evaluate  $E_N^{(b)}$  we apply (A.3) to get

$$E_N^{(b)} = -\operatorname{Im} \left( \ln \left[ \frac{a_+(is)}{(a_+(is))^*} \frac{(\bar{a}_+(-i\bar{s}))^*}{\bar{a}_+(-i\bar{s})} \right] \right)' = -\operatorname{Im} \left( \ln \left[ \frac{(\bar{a}_+(i\bar{s}))^* (\bar{a}_+(-i\bar{s}))^*}{\bar{a}_+(i\bar{s}) \bar{a}_+(-i\bar{s})} \right] \right)' = 0, \quad (\text{B.7})$$

where the last relation follows from (A.14) and (A.8). Finally, one rewrites  $E_N^{(a)}$  as

$$E_N^{(a)} = -2 \operatorname{Im} \left( \ln [\widehat{\varphi}_+(is) \widehat{\varphi}_+(i(1-s))] \right)' - 4N\psi(1), \quad (\text{B.8})$$

takes into account (4.20) and arrives at (4.25).

According to (4.24), the quasimomentum is given by

$$\theta_N = -\frac{2\pi}{N}\ell, \quad \ell = \frac{N}{\pi} \operatorname{Re} \int_{P_0^-}^{P_0^+} dx S_0'(x), \quad (\text{B.9})$$

where the ‘‘action’’ differential was defined in (3.6)<sup>7</sup>

$$dx S_0'(x) = \frac{Nt_N(x) - xt_N'(x)}{y(x)} dx. \quad (\text{B.10})$$

In Eq. (B.9) the integration contour,  $\gamma_{P_0^- P_0^+}$ , goes on the Riemann surface (1.10) from the point  $P_0^-$  located above  $x = 0$  on the lower sheet to the point  $P_0^+$  above  $x = 0$  on the upper sheet and does not intersect the cycles  $\alpha_k$  and  $\beta_k$  ( $k = 1, \dots, N - 2$ ) as shown in Figure 1.

Let us consider the following integral

$$I_k = \int_{\gamma(\sigma_k)} dx S_0'(x) = \int_{\gamma(\sigma_k)} dx \frac{Nt_N(x) - xt_N'(x)}{\sqrt{t_N^2(x) - 4x^{2N}}}. \quad (\text{B.11})$$

Here the integration contour  $\gamma(\sigma_k)$  goes from the point  $P_0^+$  above  $x = 0$  on the upper sheet of  $\Gamma_N$  to the branching point  $\sigma_k$ , encircles it and goes to the point  $P_0^-$  on the lower sheet of  $\Gamma_N$ . Notice that  $\gamma(\sigma_k)$  is different from  $\gamma_{P_0^- P_0^+}$ , but the two contours are related to each other through (3.22). It follows from (B.9) that  $\ell = N/\pi \operatorname{Re} I_k \pmod{N}$  leading to (5.5).

In general,  $I_k$  is a complicated function of the integrals of motion  $\mathbf{q}$ . The integral in (B.11) can be easily evaluated for  $\mathbf{q}$  satisfying (5.7). In that case, the spectral curve takes the form (5.8) and the branching points are given by (5.10). Replacing the integration variable in (B.11) as  $x \rightarrow u_N x$  and taking into account the hierarchy (5.9) one gets for  $j = 1, \dots, N$

$$I_j = 2u_N \int_0^{e^{i\pi(2j-1)/N}} \frac{N dx}{\sqrt{1+x^N}} \left[ 1 + \frac{1}{2} \left( \frac{x^N}{1+x^N} - \frac{2}{N} x \partial_x \right) p_{N-2}(x) + \mathcal{O}(\epsilon^2) \right], \quad (\text{B.12})$$

where  $p_{N-2}(x) = u_2 x^{N-2} + \dots + u_{N-1} x = \mathcal{O}(\epsilon)$  and we neglected terms quadratic in  $p_{N-2}(x)$ . Straightforward calculation leads to

$$I_j = 2u_N \left[ e^{i\pi(2j-1)/N} \operatorname{B}\left(\frac{1}{2}, \frac{1}{N}\right) + \frac{1}{N} \sum_{n=2}^{N-1} e^{i\pi(2j-1)n/N} u_{N+1-n} \operatorname{B}\left(\frac{1}{2}, \frac{n}{N}\right) + \mathcal{O}(\epsilon^2) \right], \quad (\text{B.13})$$

with  $\operatorname{B}(x, y) = \Gamma(x)\Gamma(y)/\Gamma(x+y)$  being the Euler function. This expression has the following properties

$$I_{j+N} = I_j, \quad \sum_{j=1}^N I_j = 0 + \mathcal{O}(\epsilon^{3/2}). \quad (\text{B.14})$$

The r.h.s. of (B.13) takes the form of a discrete Fourier transformation from the coordinate ( $j$ ) to the momentum ( $n$ ) representation. This allows one to get the moduli  $u_N$  and  $u_n$  as inverse Fourier transformation of  $I_j$ . Then, taking into account that  $\operatorname{Re} I_k = \pi(n_k + \ell/N)$ , Eq. (5.5), one arrives at (5.11).

---

<sup>7</sup>Here we neglected the last term in the r.h.s. of (3.6) since it does not contribute to (B.9).

## C Appendix: Calculation of the quasimomentum

Let us demonstrate that for the integrals of motions  $\mathbf{q}$  satisfying the quantization conditions (3.23), the parameter  $\ell$  takes strictly integer values in (B.9). To begin with, we define on the Riemann surface (1.10) the set of normalized differentials of the first kind,  $\omega_k$ , and the third kind (dipole differentials),  $\Omega_\infty$ ,

$$\omega_k = \sum_{j=1}^{N-2} U_{kj} \frac{dx x^{j-1}}{y}, \quad \Omega_\infty = 2q_2^{1/2} \frac{dx x^{N-2}}{y} + \sum_{j=1}^{N-2} U_j \frac{dx x^{j-1}}{y}, \quad (\text{C.1})$$

with the expansion coefficients  $U_{kj}$  and  $U_j$  fixed by the normalization conditions [22]

$$\oint_{\alpha_j} \omega_k = 2\pi \delta_{jk}, \quad \oint_{\alpha_j} \Omega_\infty = 0. \quad (\text{C.2})$$

The differential  $\Omega_\infty$  has a pair of poles located at the points  $(P_\infty^-, P_\infty^+)$  above  $x = \infty$  on the upper and lower sheets of  $\Gamma_N$  and the residue at these poles  $\text{res}_{P_\infty^\pm} \Omega_\infty = \pm 1$ . The action differential (B.10) can be decomposed over the set of the differentials (C.1) as

$$dx S'_0(x) = q_2^{1/2} \cdot \Omega_\infty + \sum_{k=1}^{N-2} a_k \cdot \omega_k. \quad (\text{C.3})$$

Here, the coefficient in front of  $\Omega_\infty$  is fixed by the asymptotic behaviour of  $dx S'_0(x)$ , Eq. (B.10), at infinity  $S'_0(x \rightarrow P_\infty^\pm) \sim \pm q_2^{1/2}/x$ . In the second term, the notation was introduced for the  $\alpha$ -periods of the action differential

$$a_k = \frac{1}{2\pi} \oint_{\alpha_k} dx S'_0(x), \quad \text{Re } a_k = \frac{1}{2} \ell_{2k-1}, \quad (\text{C.4})$$

whose values are fixed by the quantization conditions (3.23).

Substituting (C.3) into (B.9) and applying the well-known identities between the contour integrals on the Riemann surface [22]

$$\int_{P_0^-}^{P_0^+} \Omega_\infty = \int_{P_\infty^-}^{P_\infty^+} \Omega_0, \quad \int_{P_0^-}^{P_0^+} \omega_k = -i \oint_{\beta_k} \Omega_0, \quad (\text{C.5})$$

one can express  $\ell$  in terms of the integrals of the dipole differential  $\Omega_0$

$$\ell = \frac{N}{\pi} \text{Re} \left[ q_2^{1/2} \int_{P_\infty^-}^{P_\infty^+} \Omega_0 - i \sum_{k=1}^{N-2} a_k \oint_{\beta_k} \Omega_0 \right]. \quad (\text{C.6})$$

The differential  $\Omega_0$  has a pair of poles located at the points  $P_0^\pm$  on  $\Gamma_N$  above  $x = 0$  and is normalized as  $\oint_{\alpha_j} \Omega_0 = 0$ . This differential plays a special role in our analysis as it can be expressed in terms of the quasimomentum

$$\Omega_0 = -\frac{1}{N} dx p'(x), \quad e^{p(x)} + e^{-p(x)} = \frac{t_N(x)}{x^N}. \quad (\text{C.7})$$



Notice that  $p(x)$  is a multi-valued function on the Riemann surface (1.10) such that

$$e^{p(P_\infty^\pm)} = 1, \quad e^{p(\sigma_k)} = \pm 1, \quad (\text{C.8})$$

with  $\sigma_k$  being the edges of the cuts,  $t_N^2(\sigma_k) = 4\sigma_k^{2N}$ . As a consequence,

$$\int_{P_\infty^-}^{P_\infty^+} \Omega_0 = 2\pi i \frac{m}{N}, \quad \oint_{\beta_k} \Omega_0 = 2\pi i \frac{m_k}{N} \quad (\text{C.9})$$

with  $m$  and  $m_k$  integer. Finally, we find from (C.6)

$$\ell = 2N \operatorname{Re} \left[ i \frac{m}{N} q_2^{1/2} + \sum_{k=1}^{N-2} a_k \frac{m_k}{N} \right] = nm + 2 \sum_{k=1}^{N-2} m_k \operatorname{Re} a_k = nm + \sum_{k=1}^{N-2} m_k \ell_{2k-1}. \quad (\text{C.10})$$

Here, in the second relation we took into account that  $q_2^{1/2} = i(h - 1/2) + \mathcal{O}((h - 1/2)^{-1}) = in/2 - \nu$ , with  $h = (1+n)/2 + i\nu$ . Notice that the quasimomentum depends only on the  $\alpha$ -periods of the action differential.

## References

- [1] R.J. Baxter, *Exactly Solved Models in Statistical Mechanics*, Academic Press, London, 1982.
- [2] L.A. Takhtajan and L.D. Faddeev, *Russ. Math. Survey* **34** (1979) 11;  
E.K. Sklyanin, L.A. Takhtajan and L.D. Faddeev, *Theor. Math. Phys.* **40** (1980) 688;  
V.E. Korepin, N.M. Bogoliubov and A.G. Izergin, *Quantum inverse scattering method and correlation functions*, Cambridge Univ. Press, 1993.
- [3] P.P. Kulish, N.Y. Reshetikhin and E.K. Sklyanin, *Lett. Math. Phys.* **5** (1981) 393;  
V.O. Tarasov, L.A. Takhtajan and L.D. Faddeev, *Theor. Math. Phys.* **57** (1983) 163;  
A.N. Kirillov and N.Yu. Reshetikhin, *J. Phys. A* **20** (1987) 1565.
- [4] L.D. Faddeev, *Int. J. Mod. Phys. A* **10** (1995) 1845 [hep-th/9404013]; hep-th/9605187.
- [5] S.E. Derkachov, G.P. Korchemsky and A.N. Manashov, *Nucl. Phys. B* **617** (2001) 375 [hep-th/0107193].
- [6] L.N. Lipatov, *JETP Lett.* **59** (1994) 596 [hep-th/9311037].
- [7] L.D. Faddeev and G.P. Korchemsky, *Phys. Lett. B* **342** (1995) 311 [hep-th/9404173].
- [8] I.M. Gelfand, M.I. Graev and N.Ya. Vilenkin, *Generalized functions*, Vol. 5, Academic Press, 1966;  
D.P. Zhelobenko and A.I. Shtern, *Representations of Lie groups* (in Russian), Nauka, Moscow, 1983, pp.211-220.
- [9] G. P. Korchemsky, J. Kotanski and A. N. Manashov, *Phys. Rev. Lett.* **88** (2002) 122002 [hep-ph/0111185].

- [10] S. E. Derkachov, G. P. Korchemsky, J. Kotanski and A. N. Manashov, Nucl. Phys. B **645** (2002) 237 [hep-th/0204124].
- [11] E.K. Sklyanin, *The quantum Toda chain*, Lecture Notes in Physics, vol. 226, Springer, 1985, pp.196–233; *Functional Bethe ansatz*, in “Integrable and superintegrable systems”, ed. B.A. Kupershmidt, World Scientific, 1990, pp.8–33; *Quantum inverse scattering method. Selected topics*, “Quantum Group and Quantum Integrable Systems” (Nankai Lectures in Mathematical Physics), ed. Mo-Lin Ge, Singapore: World Scientific, 1992, pp. 63–97 [hep-th/9211111]; Progr. Theor. Phys. Suppl. **118** (1995) 35 [solv-int/9504001].
- [12] G.P. Korchemsky and I.M. Krichever, Nucl. Phys. B505 (1997) 387.
- [13] A. Gorsky, I. I. Kogan and G. Korchemsky, JHEP **0205** (2002) 053 [hep-th/0204183].
- [14] S.P. Novikov, S.V. Manakov, L.P. Pitaevskii and V.E. Zakharov, *Theory of Solitons: The Inverse Scattering Method*, Consultants Bureau, New York, 1984;  
B. Dubrovin, I. Krichever and S. Novikov, *Integrable systems - I*, Sovremennye problemy matematiki (VINITI), Dynamical systems - 4 (1985) 179;  
B.A. Dubrovin, V.B. Matveev and S.P. Novikov, Russ. Math. Surv. 31 (1976) 59;
- [15] I.M. Krichever, Russ. Math. Surv. 32 (1977) 185; Func. Anal. Appl. 14 (1980) 531; 11(1977) 12;  
I. Krichever, O. Babelon, E. Billey and M. Talon, Amer. Math. Soc. Transl. **170** (1995) 83.
- [16] V. Pasquier and M. Gaudin, J. Phys. A: Math. Gen. **25** (1992) 5243.
- [17] G. P. Korchemsky, Nucl. Phys. B **498** (1997) 68 [hep-th/9609123]; preprint LPTHE-Orsay-97-73 [hep-ph/9801377].
- [18] F.A. Smirnov, preprints LPTHE-98-10 [hep-th/9802132]; LPTHE-98-24 [math-ph/9805011]; LPTHE-00-04 [math-ph/0001032].
- [19] G.P. Korchemsky, Nucl. Phys. B **462** (1996) 333 [hep-th/9508025].
- [20] V.M. Braun, S.E. Derkachov, G.P. Korchemsky and A.N. Manashov, Nucl. Phys. B **553** (1999) 355 [hep-ph/9902375].
- [21] A. V. Belitsky, Nucl. Phys. B **574** (2000) 407 [hep-ph/9907420].
- [22] B.A. Dubrovin, Russ. Math. Surv. 36 (1981) 11.
- [23] R. Janik and J. Wosiek, Phys. Rev. Lett. **79** (1997) 2935 [hep-th/9610208]; **82** (1999) 1092 [hep-th/9802100].
- [24] H. J. De Vega and L. N. Lipatov, Phys. Rev. D **64** (2001) 114019 [hep-ph/0107225].
- [25] C.R. Ahn, V.A. Fateev, C.J. Kim, C. Rim and B. Yang, Nucl. Phys. B **565** (2000) 611 [hep-th/9907072].
- [26] H. J. de Vega and L. N. Lipatov, Phys. Rev. D **66** (2002) 074013 [hep-ph/0204245].

- [27] G.B. Whitham, *Linear and Nonlinear Waves*, John Wiley, New York, 1974;  
H. Flaschka, M.G. Forest and D.W. McLaughlin, *Comm. Pure Appl. Math.* **33** (1980) 739;  
S.Yu. Dobrokhotov and V.P. Maslov, *J. Sov. Math.* **16** (1981) 1433;  
B.A. Dubrovin and S.P. Novikov, *Russ. Math. Surv.* **44** (1989) 35.  
I.M. Krichever, *Comm. Math. Phys.* **143** (1992) 415; *Comm. Pure Appl. Math.* **47** (1994) 437;  
B.A. Dubrovin, *Comm. Math. Phys.* **145** (1992) 195.
- [28] H. Itoyama and A. Morozov, *Nucl. Phys. B* **477** (1996) 855 [hep-th/9511126] ; *Nucl. Phys. B* **491** (1997) 529 [hep-th/9512161];
- [29] N. Seiberg and E. Witten, *Nucl. Phys. B* **426** (1994) 19 [Erratum-ibid. *B* **430** (1994) 485] [hep-th/9407087]; *Nucl. Phys. B* **431** (1994) 484 [hep-th/9408099].